



Title	Instantaneous energy and enstrophy variations in Euler-alpha point vortices via triple collapse
Author(s)	Sakajo, Takashi
Citation	Journal of Fluid Mechanics, 702, 188-214 https://doi.org/10.1017/jfm.2012.172
Issue Date	2012-07-10
Doc URL	http://hdl.handle.net/2115/52952
Rights	Copyright © Cambridge University Press 2012
Type	article
File Information	JFM702_188-214.pdf



[Instructions for use](#)

Instantaneous energy and enstrophy variations in Euler-alpha point vortices via triple collapse

Takashi Sakajo†

Department of Mathematics, Hokkaido University CREST, Japan Science and Technology Agency,
Sapporo, Hokkaido, 060-0810, Japan

(Received 29 July 2011; revised 22 March 2012; accepted 6 April 2012;
first published online 21 May 2012)

It has been pointed out that the anomalous enstrophy dissipation in non-smooth weak solutions of the two-dimensional Euler equations has a clue to the emergence of the inertial range in the energy density spectrum of two-dimensional turbulence corresponding to the enstrophy cascade as the viscosity coefficient tends to zero. However, it is uncertain how non-smooth weak solutions can dissipate the enstrophy. In the present paper, we construct a weak solution of the two-dimensional Euler equations from that of the Euler- α equations proposed by Holm, Marsden & Ratiu (*Phys. Rev. Lett.*, vol. 80, 1998, pp. 4173–4176) by taking the limit of $\alpha \rightarrow 0$. To accomplish this task, we introduce the α -point-vortex (α PV) system, whose evolution corresponds to a unique global weak solution of the two-dimensional Euler- α equations in the sense of distributions (Oliver & Shkoller, *Commun. Part. Diff. Equ.*, vol. 26, 2001, pp. 295–314). Since the α PV system is a formal regularization of the point-vortex system and it is known that, under a certain special condition, three point vortices collapse self-similarly in finite time (Kimura, *J. Phys. Soc. Japan*, vol. 56, 1987, pp. 2024–2030), we expect that the evolution of three α -point vortices for the same condition converges to a singular weak solution of the Euler- α equations that is close to the triple collapse as $\alpha \rightarrow 0$, which is examined in the paper. As a result, we find that the three α -point vortices collapse to a point and then expand to infinity self-similarly beyond the critical time in the limit. We also show that the Hamiltonian energy and a kinematic energy acquire a finite jump discontinuity at the critical time, but the energy dissipation rate converges to zero in the sense of distributions. On the other hand, an enstrophy variation converges to the δ measure with a negative mass, which indicates that the enstrophy dissipates in the distributional sense via the self-similar triple collapse. Moreover, even if the special condition is perturbed, we can confirm numerically the convergence to the singular self-similar evolution with the enstrophy dissipation. This indicates that the self-similar triple collapse is a robust mechanism of the anomalous enstrophy dissipation in the sense that it is observed for a certain range of the parameter region.

Key words: Hamiltonian theory, low-dimensional models, vortex dynamics

† Email address for correspondence: sakajo@math.sci.hokudai.ac.jp

1. Introduction

1.1. Background and motivation

One of the assumptions that Kolmogorov had made in his theory of three-dimensional isotropic turbulence was that the energy dissipation rate converged to a non-zero positive constant as the kinetic viscosity coefficient ν vanished. Naively speaking, the assumption is not satisfied as long as smooth solutions of the Euler equations, which are the limit of the Navier–Stokes equations as $\nu \rightarrow 0$, are considered, since the energy dissipation rate is always zero owing to the energy conservation. On the other hand, Onsager mentioned, without any rigorous proof, that the energy could dissipate, if the Hölder continuity of non-viscous flow fields were less than or equal to $1/3$, which is known as *the Onsager conjecture* (Onsager 1949; Eyink & Sreenivasan 2006).

Constantin, E & Titi (1994) showed that the energy was conserved for a weak solution of the Euler equations in the Besov space $B_{3\infty}^\alpha(\mathbb{T}^3)$ on the three-dimensional periodic box \mathbb{T}^3 with $\alpha > 1/3$. Since the index α of the Besov space corresponds to a Hölder continuity of functions, this is regarded as a modern statement of the Onsager conjecture. Later, Duchon & Robert (2000) called a weak solution of the Euler equations *dissipative* when its corresponding energy dissipation rate was greater than or equal to zero in the sense of distribution. They showed that the energy dissipation rate was zero when the Hölder continuity of weak solutions of the Euler equations was greater than $1/3$. Also, some of the statistical properties predicted by Kolmogorov's turbulence theory are described in terms of the dissipative weak solution (Duchon & Robert 2000; Eyink 2003). These studies point out that non-smooth weak solutions of the Euler equations with the non-negative energy dissipation rate would satisfy Kolmogorov's assumption and may play a vital role in understanding of turbulence. However, the existence of dissipative weak solutions for the Euler equations is still unknown. Besides, the notion of weak solutions is so abstract that it is uncertain what kind of fluid evolution belongs to the class of dissipative weak solutions from a physical point of view. A motivation of the present study is describing such a singular weak solution as a *physically recognizable* fluid motion without losing mathematical rigour.

One procedure to construct a weak solution is regularizing the Euler equations in a certain manner and then taking the limit of their global solution with respect to the regularization parameter. As a regularized model, we consider *the Euler- α equations* proposed by Holm, Marsden & Ratiu (1998) and Holm (2002), which are derived from the Euler equations by averaging the spatial information of the flow below the small scale α (Marsden & Shkoller 2003). The three-dimensional Euler- α equations and their viscous extension, the three-dimensional Navier–Stokes- α equations, are regarded as physically relevant models of turbulent flows (Chen *et al.* 1999; Foias, Holm & Titi 2001, 2002; Mohseni *et al.* 2003). In spite of its physical significance, it is still hard to apply the procedure to the three-dimensional Euler- α equations, since the existence of a global solution for these equations is as yet unknown (Hou & Li 2006). Thus, in the present paper, we consider the two-dimensional Euler- α equations. Although the two-dimensional flow is different from the three-dimensional flow, the two-dimensional Euler- α equations provide us with more theoretical advantages than the three-dimensional ones in dealing with the present problem as explained in § 1.2. Moreover, Lunasin *et al.* (2007) confirmed numerically that the Navier–Stokes- α flow acquired the inertial ranges in the energy density spectrum that correspond to the backward energy cascade and the forward enstrophy cascade for scales larger than the filtering level α . Since the enstrophy cascade is a characteristic property observed in

two-dimensional turbulence (Kraichnan 1967; Leith 1968; Batchelor 1969), the two-dimensional Euler- α and the Navier–Stokes- α equations are also regarded as physical models of two-dimensional turbulence. Therefore, if we could construct a singular weak solution of the two-dimensional Euler- α equations that dissipates the enstrophy by taking the limit of $\alpha \rightarrow 0$, it may shed some light upon the relation between two-dimensional turbulence and singular weak solutions of the Euler equations.

1.2. The two-dimensional Euler- α and the α -point-vortex system

The Euler- α equations for the incompressible velocity field $\mathbf{u}(\mathbf{x}, t)$ in the two-dimensional space $\mathbf{x} \in \mathbb{R}^2$ and at time $t \in [0, T)$ are

$$\left. \begin{aligned} (1 - \alpha^2 \Delta) \partial_t \mathbf{u} + \mathbf{u} \cdot \nabla (1 - \alpha^2 \Delta) \mathbf{u} - \alpha^2 (\nabla \mathbf{u})^\top \cdot \Delta \mathbf{u} &= -\nabla p, \\ \nabla \cdot \mathbf{u} &= 0, \quad \mathbf{u}(\mathbf{x}, 0) = \mathbf{u}_0(\mathbf{x}). \end{aligned} \right\} \quad (1.1)$$

Introducing the scalar α -vorticity $q = (1 - \alpha^2 \Delta) \nabla^\perp \cdot \mathbf{u}$ and taking the curl of the Euler- α equations, we have the equations for q :

$$q_t + (\mathbf{u} \cdot \nabla) q = 0, \quad \mathbf{u} = K^\alpha * q, \quad q(\mathbf{x}, 0) = (1 - \alpha^2 \Delta) \nabla^\perp \cdot \mathbf{u}_0(\mathbf{x}). \quad (1.2)$$

The kernel is given by $K^\alpha(\mathbf{x}) = G^\alpha(\mathbf{x}) * (1/2\pi) \nabla^\perp \log |\mathbf{x}|$ and $G^\alpha(\mathbf{x})$ is the Green function associated with the Helmholtz operator $(1 - \alpha^2 \Delta)$,

$$G^\alpha(\mathbf{x}) = -\frac{1}{2\pi\alpha^2} \mathbf{K}_0 \left(\frac{|\mathbf{x}|}{\alpha} \right), \quad (1.3)$$

in which $\mathbf{K}_0(x)$ is a modified Bessel function of the second kind (Watson 2008).

Linshiz & Titi (2010) showed that there existed a unique global solution of the two-dimensional Euler- α equations for the initial velocity field in the Sobolev space $H^m(\mathbb{R}^2)$, $m > 2$, and it converged to that of the Euler equations in $L^\infty([0, \infty); H^m)$. Moreover, for weaker initial vorticity data in the space of Radon measure on \mathbb{R}^2 , the global existence of a unique weak solution in the sense of distributions has been established by Oliver & Shkoller (2001). On the other hand, in a similar manner as in the three-dimensional Euler equations, Duchon & Robert (2000) defined a weak solution of the two-dimensional Euler equations with non-negative energy dissipation rate in the distributional sense. They also showed that the weak solution for the initial vorticity data in $L^p(\mathbb{R}^2) \cap L^1(\mathbb{R}^2)$, whose existence has been proven by Diperna & Majda (1987), was not dissipative if $p > 3/2$. Moreover, Eyink (2001) proved that the weak solution did not dissipate the enstrophy for $1 < p < \infty$ in a weak sense. Therefore, we need to consider weaker function spaces for the initial vorticity data in order to obtain weak solutions with enstrophy dissipation.

When the vorticity field is represented by discrete δ -functions, a point-vortex system is derived from the two-dimensional Euler- α equations, which we call *the α -point-vortex (α PV) system*. The α -point vortex was first introduced by Holm & Marsden (1998) and its induced velocity field was derived by Holm, Nitsche & Putkaradze (2006). The α PV system provides us with an important class of global weak solutions of the Euler- α equations, since the vorticity field consisting of discrete δ -functions belongs to the space of Radon measure on \mathbb{R}^2 . This contrasts with the fact that the motion of point vortices, which is formally reduced from the Euler equations for the discrete vorticity field, is not a weak solution of the Euler equations, since the velocity field induced by the point vortices does not belong to $L^2_{loc}(\mathbb{R}^2)$ in which a weak solution of the Euler equations exists (Delrois 1991).

It is also known that, under a certain circumstance, three point vortices collide self-similarly at a point in finite time (Aref 1979; Novikov & Sedov 1979; Kimura 1987). Since the Euler equations are formally equivalent to the Euler- α equations with $\alpha = 0$, one can expect that, under the same circumstance, the motion of three α -point vortices converges to a singular solution that is close to the triple collapse as α tends to zero, which is examined in the present paper. Strictly speaking, since the motion of the α -point vortices for $\alpha \rightarrow 0$ is different from that of the point vortices, the triple collapse is just a reference to obtain a singular weak solution of the Euler- α equations. It is also worth mentioning that the triple collapse of the point vortex itself is less important as long as we are concerned with the relation between singular weak solutions and two-dimensional turbulence, since the triple collapse is not a weak solution of the Euler equations. Hence, the singular weak solution of the Euler- α equations for $\alpha \rightarrow 0$ is a mathematical entity that could dissipate the enstrophy. This is the reason why we consider the limit solution of the α PV system.

In the next section, we give a brief summary of some known results on the point-vortex system that help the reader understand the following sections. In §3, the equation of α -point vortices is derived from the Euler- α equations. Then, we show that the α PV system satisfies a scaling property that reduces the system to a canonical one. We also give an energy and an enstrophy that vary with the evolution of α -point vortices. In §4, we describe the evolution of three α -point vortices under the same condition as that for the self-similar triple collapse of the point vortices. We consider the behaviour of the three α -point vortices as $\alpha \rightarrow 0$, with which we observe how the Hamiltonian energy, the energy and the enstrophy change in time in the limit. The final section is summary and discussion.

2. A brief review on the point-vortex system

Let us introduce some of the known results on the point-vortex system, which are required to describe the motion of α -point vortices in the following sections. The reader can find more details and references in the book of Newton (2001). Suppose that N point vortices with strengths Γ_m are located at $\mathbf{x}_m(t) = (x_m(t), y_m(t))$ for $m = 1, \dots, N$ in the unbounded two-dimensional space \mathbb{R}^2 . Then the evolution of the point vortices is described by the following Hamiltonian dynamical system:

$$\frac{dx_m}{dt} = \{x_m, H_p\} = -\frac{1}{2\pi} \sum_{n \neq m}^N \Gamma_n \frac{y_m - y_n}{l_{mn}^2}, \quad \frac{dy_m}{dt} = \{y_m, H_p\} = \frac{1}{2\pi} \sum_{n \neq m}^N \Gamma_n \frac{x_m - x_n}{l_{mn}^2}, \quad (2.1)$$

for $m = 1, \dots, N$, in which the Hamiltonian H_p is given by

$$H_p = -\frac{1}{2\pi} \sum_{m=1}^N \sum_{n=m+1}^N \Gamma_m \Gamma_n \log |\mathbf{x}_m - \mathbf{x}_n|, \quad (2.2)$$

and the Poisson bracket between two functions f and g is defined by

$$\{f, g\} = \sum_{m=1}^N \frac{1}{\Gamma_m} \left(\frac{\partial f}{\partial x_m} \frac{\partial g}{\partial y_m} - \frac{\partial g}{\partial x_m} \frac{\partial f}{\partial y_m} \right). \quad (2.3)$$

Identifying $z_m(t) = x_m(t) + iy_m(t) \in \mathbb{C}$, we rewrite (2.1) in the following complex form:

$$\frac{dz_m^*}{dt} = \frac{1}{2\pi i} \sum_{n \neq m}^N \frac{\Gamma_n}{z_m - z_n}, \quad (2.4)$$

in which z^* denotes the complex conjugate of z and $i = \sqrt{-1}$. Let us now define the linear impulse $L \in \mathbb{C}$ and the angular momentum $I \in \mathbb{R}$ by

$$L = Q + iP = \sum_{m=1}^N \Gamma_m z_m, \quad I = \sum_{m=1}^N \Gamma_m |z_m|^2. \quad (2.5)$$

Since $\{P^2 + Q^2, H\} = 0$ and $\{I, H\} = 0$, they are invariant quantities. Moreover, we have $\{P^2 + Q^2, I\} = 0$ and thus the point-vortex system (2.1) with $N = 3$ is integrable. It is also integrable for $N = 4$ when the total vortex strength is zero, i.e. $\Gamma \equiv \sum_{m=1}^N \Gamma_m = 0$, because of $\{Q, I\} = P$, $\{P, I\} = Q$ and $\{Q, P\} = \Gamma$.

It is sometimes convenient to consider the evolution of the distance $l_{mn} = |\mathbf{x}_m - \mathbf{x}_n|$ between two point vortices at \mathbf{x}_m and \mathbf{x}_n . Its governing equation is given by

$$\frac{d}{dt} l_{mn}^2 = \frac{2}{\pi} \sum_{k \neq m \neq n}^N \Gamma_k \sigma_{mnk} A_{mnk} \left(\frac{1}{l_{nk}^2} - \frac{1}{l_{km}^2} \right), \quad (2.6)$$

where σ_{mnk} and A_{mnk} symbolize the arrangement and the area of the triangle formed by the three point vortices at \mathbf{x}_m , \mathbf{x}_n and \mathbf{x}_k respectively. The arrangement σ_{mnk} is $+1$ if the order of the indices m, n, k is counterclockwise, and it is -1 if they are clockwise. The area A_{mnk} is represented by

$$A_{mnk} = \frac{1}{4} [2 (l_{mn}^2 l_{nk}^2 + l_{nk}^2 l_{km}^2 + l_{km}^2 l_{mn}^2) - l_{mn}^4 - l_{nk}^4 - l_{km}^4]^{1/2}. \quad (2.7)$$

Note that the invariant quantities are rewritten in terms of the distance:

$$H_p = -\frac{1}{2\pi} \sum_{m=1}^N \sum_{n=m+1}^N \Gamma_m \Gamma_n \log l_{mn}, \quad M \equiv \sum_{m=1}^N \sum_{n=m+1}^N \Gamma_m \Gamma_n l_{mn}^2 = \Gamma I - Q^2 - P^2. \quad (2.8)$$

The energy generated by the evolution of the N point vortices was derived by Novikov (1976). Since the vorticity field generated by the N point vortices at $\mathbf{x}_m(t)$ for $m = 1, \dots, N$ is represented by

$$\omega(\mathbf{x}, t) = \sum_{m=1}^N \Gamma_m \delta(\mathbf{x} - \mathbf{x}_m(t)), \quad (2.9)$$

in the sense of distributions, its Fourier transform is given by

$$\widehat{\omega}(\boldsymbol{\xi}, t) = \frac{1}{2\pi} \sum_{m=1}^N \Gamma_m \exp[-i\boldsymbol{\xi} \cdot \mathbf{x}_m(t)], \quad (2.10)$$

which yields the magnitude of the spectrum,

$$|\widehat{\omega}(\boldsymbol{\xi}, t)|^2 = \frac{1}{4\pi^2} \left[\sum_{m=1}^N \Gamma_m^2 + 2 \sum_{m=1}^N \sum_{n=m+1}^N \Gamma_m \Gamma_n \cos(\boldsymbol{\xi} \cdot (\mathbf{x}_m - \mathbf{x}_n)) \right]. \quad (2.11)$$

Let $\widehat{\mathbf{v}}(\boldsymbol{\xi}, t)$ denote the Fourier transform of the velocity field $\mathbf{v}(\mathbf{x}, t)$ induced by the vorticity field (2.9). Then we obtain the total energy,

$$\frac{1}{2} \int_{\mathbb{R}^2} |\widehat{\mathbf{v}}(\boldsymbol{\xi}, t)|^2 d\boldsymbol{\xi} = \frac{1}{2} \int_0^\infty \int_{-\pi}^\pi |\widehat{\mathbf{v}}(\boldsymbol{\xi}, t)|^2 \xi d\xi d\theta = \int_0^\infty \pi \xi \langle |\widehat{\mathbf{v}}(\boldsymbol{\xi}, t)|^2 \rangle d\xi, \quad (2.12)$$

in which $\xi = |\xi|$ and $\langle f(\cdot) \rangle = (1/2\pi) \int_{-\pi}^{\pi} f(\theta) d\theta$ denotes the average of the function $f(\theta)$ with respect to the angle variable θ . Thus the energy density spectrum is represented by

$$\begin{aligned} E_N(\xi, t) &= \pi\xi \langle |\widehat{v}(\xi, t)|^2 \rangle = \frac{\pi}{\xi} \langle |\widehat{\omega}(\xi, t)|^2 \rangle \\ &= \frac{1}{4\pi\xi} \left[\sum_{m=1}^N \Gamma_m^2 + 2 \sum_{m=1}^N \sum_{n=m+1}^N \Gamma_m \Gamma_n J_0(\xi l_{mn}) \right], \end{aligned} \quad (2.13)$$

in which $J_0(x)$ is a Bessel function. Hence, the total energy from a small scale $0 < l \ll 1$ to a large scale $1 \ll L < \infty$ is given by

$$\begin{aligned} \int_{L^{-1}}^{l^{-1}} E_N(\xi, t) d\xi &= \frac{1}{4\pi} \sum_{m=1}^N \Gamma_m^2 \log \frac{l}{L} + \frac{1}{2\pi} \sum_{m=1}^N \sum_{n=m+1}^N \Gamma_m \Gamma_n \int_{L^{-1}}^{l^{-1}} \frac{J_0(\xi l_{mn})}{\xi} d\xi \\ &\sim \frac{1}{4\pi} \sum_{m=1}^N \Gamma_m^2 \log \frac{l}{L} + \frac{1}{2\pi} \sum_{m=1}^N \sum_{n=m+1}^N \Gamma_m \Gamma_n \log \frac{LC_1}{l_{mn}}, \end{aligned} \quad (2.14)$$

where $C_1 = 2e^{-\gamma}$, and γ is the Euler number.

Since the scales l and L are fixed, the first term of (2.14) is constant in time. Thus, the non-constant part of the total energy, say $E_p(t)$, is described by the second term,

$$E_p(t) \equiv -\frac{1}{2\pi} \sum_{m=1}^N \sum_{n=m+1}^N \Gamma_m \Gamma_n \log l_{mn}(t). \quad (2.15)$$

This is equivalent to the Hamiltonian H_p of the point-vortex system, which is conserved for solutions of (2.1).

In what follows, let us recall a special singular solution appearing in the integrable motion of three point vortices with the following additional conditions:

$$\frac{1}{\Gamma_1} + \frac{1}{\Gamma_2} + \frac{1}{\Gamma_3} = 0, \quad M = \Gamma_1 \Gamma_2 l_{12}^2 + \Gamma_2 \Gamma_3 l_{23}^2 + \Gamma_3 \Gamma_1 l_{31}^2 = 0. \quad (2.16)$$

Then, it is shown that three point vortices collide self-similarly at a point in finite time unless their configuration is an equilibrium (Aref 1979; Novikov & Sedov 1979; Newton 2001). Kimura (1987) constructed the self-similar collapsing solution by assuming that the orbits of the point vortices are expressed by $z_m(t) = \lambda_m f(t)$ for $m = 1, 2, 3$, in which $\lambda_m \in \mathbb{C}$ are complex constants and $f(t) = r(t) \exp(i\vartheta(t))$ is a complex-valued function. Substituting the expression $z_m(t) = \lambda_m f(t)$ into (2.4), we have the differential equation for $f(t)$,

$$f^* \frac{df}{dt} = C \equiv \mathcal{A} + i\mathcal{B}, \quad (2.17)$$

where $C \in \mathbb{C}$ and $\mathcal{A}, \mathcal{B} \in \mathbb{R}$, and the algebraic equation for λ_m is

$$\lambda_m C = \frac{i}{2\pi} \sum_{n \neq m}^3 \frac{\Gamma_n}{\lambda_m^* - \lambda_n^*}. \quad (2.18)$$

Equation (2.17) is further reduced to those for $r(t)$ and $\vartheta(t)$ as follows:

$$\frac{d}{dt} r^2 = 2\mathcal{A}, \quad \frac{d}{dt} \vartheta = \frac{\mathcal{B}}{r^2}. \quad (2.19)$$

When $\mathcal{A} = 0$, the solutions are $r(t) = 1$ and $\vartheta(t) = \mathcal{B}t$ for the initial data $r(0) = 1$ and $\vartheta(0) = 0$, which correspond to a relative equilibrium rotating at the constant speed \mathcal{B} . On the other hand, for $\mathcal{A} \neq 0$, when we consider the initial conditions

$$r\left(\frac{1}{2\mathcal{A}}\right) = 1, \quad \vartheta\left(\frac{1}{2\mathcal{A}}\right) = 0, \quad (2.20)$$

the solution of the differential equation (2.17) is given by

$$r(t) = \sqrt{2\mathcal{A}t}, \quad \vartheta(t) = \frac{\mathcal{B}}{2\mathcal{A}} \log(2\mathcal{A}t). \quad (2.21)$$

This indicates that, for $\mathcal{A} < 0$, the motion of the three point vortices is defined for $t < 0$ and they approach each other from infinity and collapse self-similarly at the origin at $t = 0$, which we refer to as *the triple collapse*. On the other hand, for $\mathcal{A} > 0$, the point vortices emerge from the origin at $t = 0$ and expand self-similarly towards infinity, which we call *the triple expansion*. The constants \mathcal{A} and \mathcal{B} are determined by solving the algebraic equation (2.18) with respect to λ_m . Kimura (1987) also gave the initial configurations of the three point vortices that satisfy (2.18) for which \mathcal{A} changes its sign. This proves the existence of the self-similar singular solutions.

3. The α -point-vortex (α PV) system

3.1. General formulations

Let us assume that the α -vorticity field $q(\mathbf{x}, t)$ is represented by N discrete δ -functions, say α -point vortices, with strength Γ_n located at $\mathbf{x}_n(t) = (x_n(t), y_n(t)) \in \mathbb{R}^2$ for $n = 1, \dots, N$,

$$q(\mathbf{x}, t) = \sum_{n=1}^N \Gamma_n \delta(\mathbf{x} - \mathbf{x}_n(t)). \quad (3.1)$$

The explicit representation of the kernel $K^\alpha(\mathbf{x})$ in (1.2) is provided by Holm *et al.* (2006):

$$K^\alpha(\mathbf{x}) = -\frac{1}{2\pi} \nabla^\perp \left[\log |\mathbf{x}| + \text{K}_0 \left(\frac{|\mathbf{x}|}{\alpha} \right) \right]. \quad (3.2)$$

Substituting (3.1) into $\mathbf{u} = K^\alpha * q$ and evaluating the velocity at $\mathbf{x} = \mathbf{x}_m(t)$, we derive the equations for the α -point vortices.

$$\frac{dx_m}{dt} = -\frac{1}{2\pi} \sum_{n \neq m}^N \Gamma_n \frac{y_m - y_n}{l_{mn}^2} B_K \left(\frac{l_{mn}}{\alpha} \right), \quad \frac{dy_m}{dt} = \frac{1}{2\pi} \sum_{n \neq m}^N \Gamma_n \frac{x_m - x_n}{l_{mn}^2} B_K \left(\frac{l_{mn}}{\alpha} \right), \quad (3.3)$$

where $l_{mn} = |\mathbf{x}_m - \mathbf{x}_n|$ and $B_K(x) = 1 - x\text{K}_1(x)$. The function $\text{K}_1(x)$ is a modified Bessel function of the second kind (Watson 2008). We call the system (3.3) *the α -point-vortex (α PV) system*. Since $B_K(x) \rightarrow 1$ owing to $\text{K}_1(x) \rightarrow e^{-x}$ as $x \rightarrow \infty$, the α PV system for $\alpha \rightarrow 0$ is formally equivalent to the point-vortex system (2.1). On the other hand, we have $B_K(x) \rightarrow 0$ for $x \rightarrow 0$, since $\text{K}_1(x) \sim 1/x$ as $x \rightarrow 0$. Thus the velocity field vanishes when the distance between two α -point vortices tends to zero, which means that the velocity field is regularized thanks to the function $B_K(l_{mn}/\alpha)$, in which the function $B_K(x)$ is monotonically increasing for $x > 0$, since

$$\frac{d}{dx} B_K(x) = -\text{K}_1(x) - x \frac{d}{dx} \text{K}_1(x) = x\text{K}_0(x) > 0. \quad (3.4)$$

This is a dispersive regularization of the point-vortex system. Note that a dissipative regularized point-vortex model is proposed by Shashikanth (2010). It is important to remember that the solution of the α PV system corresponds to a global weak solution of the Euler- α equations for the initial data in the space of Radon measure on \mathbb{R}^2 , to which the vorticity field (3.1) belongs. Consequently, there exists no finite-time collapse in the α PV system.

In the same spirit as Novikov's derivation, we derive an energy that evolves with the motion of α -point vortices. Since the α -vorticity is defined by $q = (1 - \alpha^2 \Delta) \nabla^\perp \cdot \mathbf{u}$ and it is represented by (3.1), the energy density spectrum is given by

$$\begin{aligned} E_N^{(\alpha)}(\xi, t) &= \pi \xi \langle |\widehat{\mathbf{u}}(\xi, t)|^2 \rangle = \frac{\pi}{(1 + \alpha^2 \xi^2)^2 \xi} \langle |\widehat{q}(\xi, t)|^2 \rangle \\ &= \frac{1}{4\pi (1 + \alpha^2 \xi^2)^2 \xi} \left[\sum_{m=1}^N \Gamma_m^2 + 2 \sum_{m=1}^N \sum_{n=m+1}^N \Gamma_m \Gamma_n J_0(\xi l_{mn}) \right]. \end{aligned} \quad (3.5)$$

Hence, the total energy becomes

$$\begin{aligned} \int_{L^{-1}}^{l^{-1}} E_N^{(\alpha)}(\xi, t) d\xi &= \frac{1}{4\pi} \sum_{m=1}^N \Gamma_m^2 \int_{L^{-1}}^{l^{-1}} \frac{d\xi}{(1 + \alpha^2 \xi^2)^2 \xi} \\ &\quad + \frac{1}{2\pi} \sum_{m=1}^N \sum_{n=m+1}^N \Gamma_m \Gamma_n \int_{L^{-1}}^{l^{-1}} \frac{J_0(\xi l_{mn})}{(1 + \alpha^2 \xi^2)^2 \xi} d\xi. \end{aligned} \quad (3.6)$$

The integral in the second term is evaluated as follows:

$$\begin{aligned} \int_{L^{-1}}^{l^{-1}} \frac{J_0(\xi l_{mn})}{(1 + \alpha^2 \xi^2)^2 \xi} d\xi &= \int_{L^{-1}}^{l^{-1}} \frac{J_0(\xi l_{mn})}{\xi} d\xi - \int_{L^{-1}}^{l^{-1}} \frac{\alpha^2 \xi J_0(\xi l_{mn})}{1 + \alpha^2 \xi^2} d\xi \\ &\quad - \int_{L^{-1}}^{l^{-1}} \frac{\alpha^2 \xi J_0(\xi l_{mn})}{(1 + \alpha^2 \xi^2)^2} d\xi \\ &\sim \log \frac{LC_1}{l_{mn}} - K_0 \left(\frac{l_{mn}}{\alpha} \right) - \frac{l_{mn}}{2\alpha} K_1 \left(\frac{l_{mn}}{\alpha} \right), \end{aligned} \quad (3.7)$$

in which the following formulae in terms of Bessel functions are used (Watson 2008):

$$\left. \begin{aligned} \int_0^\infty \frac{x J_0(ax)}{1 + x^2} dx &= K_0(a), \\ \int_0^\infty \frac{x^{v+1} J_v(ax)}{(1 + x^2)^{\mu+1}} dx &= \frac{a^\mu K_{v-\mu}(a)}{2^\mu \Gamma(\mu + 1)}, \quad \mu + 3/2 > v > -1. \end{aligned} \right\} \quad (3.8)$$

Removing the constant terms, we have the non-constant part of the energy $E^{(\alpha)}(t)$ that varies with the evolution of α -point vortices:

$$E^{(\alpha)}(t) = -\frac{1}{2\pi} \sum_{m=1}^N \sum_{n=m+1}^N \Gamma_m \Gamma_n \left[\log l_{mn}(t) + K_0 \left(\frac{l_{mn}(t)}{\alpha} \right) + \frac{l_{mn}(t)}{2\alpha} K_1 \left(\frac{l_{mn}(t)}{\alpha} \right) \right]. \quad (3.9)$$

Another important quantity is the enstrophy, which is the L^2 norm of the vorticity field. Here, we define the part of the enstrophy that evolves with the motion of α -point vortices in the sense of Novikov. Since $\widehat{q}(\xi, t) = (1 + \alpha^2 \xi^2) \widehat{\omega}(\xi, t)$ owing

to $q = (1 - \alpha^2 \Delta)\omega$, the enstrophy density spectrum is described by

$$\begin{aligned} \mathcal{L}_N^{(\alpha)}(\xi, t) &\equiv \frac{\pi \xi}{(1 + \alpha^2 \xi^2)^2} \langle |\widehat{q}(\xi, t)|^2 \rangle \\ &= \frac{\xi}{4\pi (1 + \alpha^2 \xi^2)^2} \left[\sum_{m=1}^N \Gamma_m^2 + 2 \sum_{m=1}^N \sum_{n=m+1}^N \Gamma_m \Gamma_n J_0(\xi l_{mn}) \right]. \end{aligned} \quad (3.10)$$

Integrating it from the scale l to L , we have

$$\begin{aligned} \int_{L^{-1}}^{l^{-1}} \mathcal{L}_N^{(\alpha)}(\xi, t) \, d\xi &= \frac{1}{4\pi} \sum_{m=1}^N \Gamma_m^2 \int_{L^{-1}}^{l^{-1}} \frac{\xi}{(1 + \alpha^2 \xi^2)^2} \, d\xi \\ &\quad + \frac{1}{2\pi} \sum_{m=1}^N \sum_{n=m+1}^N \Gamma_m \Gamma_n \int_{L^{-1}}^{l^{-1}} \frac{\xi J_0(\xi l_{mn})}{(1 + \alpha^2 \xi^2)^2} \, d\xi. \end{aligned} \quad (3.11)$$

The second term is the non-constant part of the enstrophy, say $\mathcal{Z}^{(\alpha)}(t)$. On use of (3.8), it is represented by

$$\mathcal{Z}^{(\alpha)}(t) = \frac{1}{4\pi \alpha^2} \sum_{m=1}^N \sum_{n=m+1}^N \frac{l_{mn}(t)}{\alpha} \mathbf{K}_1 \left(\frac{l_{mn}(t)}{\alpha} \right). \quad (3.12)$$

3.2. Canonical system and integrability

Introducing the scaled variables $\mathbf{X}_m(t) = (X_m(t), Y_m(t))$ and $L_{mn}(t)$ with

$$X_m(t) = \frac{1}{\alpha} x_m(\alpha^2 t), \quad Y_m(t) = \frac{1}{\alpha} y_m(\alpha^2 t), \quad L_{mn}(t) = |\mathbf{X}_m(t) - \mathbf{X}_n(t)| = \frac{1}{\alpha} l_{mn}(\alpha^2 t), \quad (3.13)$$

we have the equations for $\mathbf{X}_m(t)$:

$$\frac{d\mathbf{X}_m}{dt} = -\frac{1}{2\pi} \sum_{n \neq m}^N \Gamma_n \frac{Y_m - Y_n}{L_{mn}^2} \mathbf{B}_K(L_{mn}), \quad \frac{dY_m}{dt} = \frac{1}{2\pi} \sum_{n \neq m}^N \Gamma_n \frac{X_m - X_n}{L_{mn}^2} \mathbf{B}_K(L_{mn}). \quad (3.14)$$

Note that equations (3.14) are equivalent to (3.3) with $\alpha = 1$. Since the solution of (3.3) is recovered from $X_m(t)$, $Y_m(t)$ and $L_{mn}(t)$ by

$$x_m(t) = \alpha X_m(t/\alpha^2), \quad y_m(t) = \alpha Y_m(t/\alpha^2), \quad l_{mn}(t) = \alpha L_{mn}(t/\alpha^2), \quad (3.15)$$

(3.14) can be regarded as a canonical system for the α PV system.

We give some equivalent expressions to (3.14), which are used in the present paper. The canonical system is a Hamiltonian dynamical system with the same Poisson bracket as (2.3) and the Hamiltonian $H = H_0(t) + H_1(t)$, in which

$$\left. \begin{aligned} H_0(t) &= -\frac{1}{2\pi} \sum_{m=1}^N \sum_{n=m+1}^N \Gamma_m \Gamma_n \log L_{mn}(t), \\ H_1(t) &= -\frac{1}{2\pi} \sum_{m=1}^N \sum_{n=m+1}^N \Gamma_m \Gamma_n \mathbf{K}_0(L_{mn}(t)). \end{aligned} \right\} \quad (3.16)$$

We note that the two terms H_0 and H_1 can exchange their values during the evolution of the α -point vortices, although their total sum H remains constant for all time. The

complex representation of (3.14) becomes

$$\frac{dZ_m^*}{dt} = \frac{1}{2\pi i} \sum_{n \neq m}^N \frac{\Gamma_n}{Z_m - Z_n} B_K(|Z_m - Z_n|), \quad (3.17)$$

where $Z_m(t) = X_m(t) + iY_m(t)$. The equation for the distance L_{mn} is

$$\frac{d}{dt} L_{mn}^2 = \frac{2}{\pi} \sum_{k \neq m \neq n}^N \Gamma_k \sigma_{mnk} A_{mnk} \left(\frac{1}{L_{nk}^2} B_K(L_{nk}) - \frac{1}{L_{km}^2} B_K(L_{km}) \right), \quad (3.18)$$

where σ_{mnk} and A_{mnk} are the same as those defined in § 2.

Let us discuss the integrability of the canonical system as in Aref (1979) and Newton (2001). The linear impulse L and the angular momentum I defined as in (2.5) are again invariant quantities for the canonical system, since

$$\begin{aligned} \frac{dL}{dt} &= \sum_{m=1}^N \Gamma_m \frac{dZ_m}{dt} = - \sum_{m=1}^N \Gamma_m \sum_{n \neq m}^N \frac{\Gamma_n}{2\pi i} \frac{1}{Z_m^* - Z_n^*} B_K(|Z_m - Z_n|) \\ &= - \sum_{m=1}^N \sum_{n=m+1}^N \frac{\Gamma_m \Gamma_n}{2\pi i} \frac{1}{Z_m^* - Z_n^*} B_K(|Z_m - Z_n|) + \sum_{n=1}^N \sum_{m=n+1}^N \frac{\Gamma_m \Gamma_n}{2\pi i} \frac{1}{Z_n^* - Z_m^*} B_K(|Z_m - Z_n|) \\ &= 0, \end{aligned} \quad (3.19)$$

and

$$\begin{aligned} \frac{dI}{dt} &= - \frac{1}{2\pi i} \left(\sum_{m=1}^N \sum_{n=m+1}^N \frac{\Gamma_m \Gamma_n Z_m^*}{Z_m^* - Z_n^*} B_K(|Z_m - Z_n|) - \sum_{n=1}^N \sum_{m=n+1}^N \frac{\Gamma_m \Gamma_n Z_m^*}{Z_n^* - Z_m^*} B_K(|Z_m - Z_n|) \right) \\ &\quad + \frac{1}{2\pi i} \left(\sum_{m=1}^N \sum_{n=m+1}^N \frac{\Gamma_m \Gamma_n Z_m}{Z_m - Z_n} B_K(|Z_m - Z_n|) - \sum_{n=1}^N \sum_{m=n+1}^N \frac{\Gamma_m \Gamma_n Z_m}{Z_n - Z_m} B_K(|Z_m - Z_n|) \right) \\ &= - \frac{1}{2\pi i} \sum_{m=1}^N \sum_{n=m+1}^N \Gamma_m \Gamma_n B_K(|Z_m - Z_n|) + \frac{1}{2\pi i} \sum_{m=1}^N \sum_{n=m+1}^N \Gamma_m \Gamma_n B_K(|Z_m - Z_n|) \\ &= 0. \end{aligned} \quad (3.20)$$

Hence, $M = \Gamma I - Q^2 - P^2 = \sum_{m=1}^N \sum_{n=m+1}^N \Gamma_m \Gamma_n L_{mn}^2$ is also conserved. Since the definitions of L , I and the Poisson bracket are the same as those introduced in the point-vortex system of § 2, we also have $\{P^2 + Q^2, I\} = 0$, $\{Q, P\} = \Gamma$, $\{Q, I\} = P$ and $\{P, I\} = Q$. Accordingly, the α PV system for $N \leq 3$ is integrable for all values of Γ_m . Furthermore, if the total strength of the vortices is zero, i.e. $\Gamma = 0$, it is integrable for $N = 4$.

4. A three- α -vortex problem

4.1. Long-time evolution

We consider an integrable α PV system for $N = 3$ subject to the same additional conditions as (2.16):

$$\frac{1}{\Gamma_1} + \frac{1}{\Gamma_2} + \frac{1}{\Gamma_3} = 0, \quad (4.1)$$

$$M = \Gamma_1 \Gamma_2 L_{12}^2 + \Gamma_2 \Gamma_3 L_{23}^2 + \Gamma_3 \Gamma_1 L_{31}^2 = 0. \quad (4.2)$$

The analytical techniques used here are the same as those used by Synge (1949), Aref (1979) and Newton (2001), but there are some mathematical difficulties owing to the presence of the regularization term $B_K(x)$ in the α PV system. The following analysis will facilitate the construction of a singular weak solution of the Euler- α equations by taking limit of $\alpha \rightarrow 0$ rigorously in §4.2. Owing to (4.1), we may assume that $\Gamma_1 \geq \Gamma_2 > 0 > \Gamma_3$ without loss of generality. Equation (3.18) for the distance L_{mn} is explicitly written as

$$\frac{d}{dt}L_{12}^2 = \frac{2}{\pi} \Gamma_3 A \left[\frac{1}{L_{23}^2} B_K(L_{23}) - \frac{1}{L_{31}^2} B_K(L_{31}) \right], \tag{4.3}$$

$$\frac{d}{dt}L_{23}^2 = \frac{2}{\pi} \Gamma_1 A \left[\frac{1}{L_{31}^2} B_K(L_{31}) - \frac{1}{L_{12}^2} B_K(L_{12}) \right], \tag{4.4}$$

$$\frac{d}{dt}L_{31}^2 = \frac{2}{\pi} \Gamma_2 A \left[\frac{1}{L_{12}^2} B_K(L_{12}) - \frac{1}{L_{23}^2} B_K(L_{23}) \right], \tag{4.5}$$

where $A = \sigma_{123}A_{123} = \sigma_{231}A_{231} = \sigma_{312}A_{312}$ denotes the signed area of the triangle formed by the three α -point vortices. It is computed from Heron’s formula,

$$A^2 = r(r - L_{12})(r - L_{23})(r - L_{31}), \quad r = \frac{1}{2}(L_{12} + L_{23} + L_{31}), \tag{4.6}$$

and its magnitude $|A|$ is expressed by

$$|A| = \frac{1}{4} [2(L_{12}^2 L_{23}^2 + L_{23}^2 L_{31}^2 + L_{31}^2 L_{12}^2) - L_{12}^4 - L_{23}^4 - L_{31}^4]^{1/2} \geq 0, \tag{4.7}$$

which is equivalent to (2.7). The signed area evolves according to the motion of the three α -point vortices, whose governing equation is obtained by differentiating (4.6) and plugging (4.3)–(4.5) into it:

$$\begin{aligned} \frac{dA}{dt} &= \frac{1}{4\pi} \sum \Gamma_1 L_{23}^{-1} [L_{31}^{-2} B_K(L_{31}) - L_{12}^{-2} B_K(L_{12})] \\ &\quad \times \left[(r - L_{23})(r - L_{31})(r - L_{12}) + r \sum (r - L_{31})(r - L_{12}) \right] \\ &\quad - \frac{r}{2\pi} \sum \Gamma_1 L_{23}^{-1} [L_{31}^{-2} B_K(L_{31}) - L_{12}^{-2} B_K(L_{12})] (r - L_{31})(r - L_{12}), \end{aligned} \tag{4.8}$$

in which \sum denotes the summation over cyclic permutation of indices, for instance $\sum L_{12} = L_{12} + L_{23} + L_{31}$. Equations (4.3)–(4.5) and (4.8) define a four-dimensional dynamical system for $(L_{12}, L_{23}, L_{31}, A)$. Since M is invariant, it is further reduced to the two-dimensional system for L_{23} and L_{31} . Thus we first determine the range where the variables (L_{23}, L_{31}) can exist. It follows from (4.1) and (4.2) that

$$L_{12}^2 = -\frac{\Gamma_3}{\Gamma_1} L_{23}^2 - \frac{\Gamma_3}{\Gamma_2} L_{31}^2 = \frac{\Gamma_1 + k\Gamma_2}{\Gamma_1 + \Gamma_2} L_{31}^2. \tag{4.9}$$

Let us write $L_{23}^2/L_{31}^2 = k$. Then (4.7) is equivalent to

$$k^2 + 1 + \left(\frac{\Gamma_1 + k\Gamma_2}{\Gamma_1 + \Gamma_2} \right)^2 - 2k - 2 \frac{\Gamma_1 + k\Gamma_2}{\Gamma_1 + \Gamma_2} - 2k \frac{\Gamma_1 + k\Gamma_2}{\Gamma_1 + \Gamma_2} \leq 0, \tag{4.10}$$

which yields the quadratic inequality for k ,

$$f(k) \equiv \Gamma_1^2 k^2 - 2(2\Gamma_1^2 + 3\Gamma_1\Gamma_2 + 2\Gamma_2^2)k + \Gamma_2^2 \leq 0. \tag{4.11}$$

Since the determinant of the equation $f(k) = 0$ is $4(\Gamma_1^2 + 2\Gamma_1\Gamma_2 + \Gamma_2^2)(\Gamma_1^2 + \Gamma_1\Gamma_2 + \Gamma_2^2) > 0$, there are two real solutions of $f(k) = 0$, say k_1 and k_2 . Furthermore, owing to $f(0) = \Gamma_2^2 > 0$ and $f(1) = -3(\Gamma_1 + \Gamma_2)^2 < 0$, we have $0 < k_1 < 1 < k_2$. Hence, $|A| \geq 0$ is equivalent to $k_1 \leq L_{23}^2/L_{31}^2 \leq k_2$, in which (L_{23}, L_{31}) can exist.

Next, we investigate equilibria of (4.3)–(4.5) and (4.8). It follows from (4.3)–(4.5) that $dL_{23}^2/dt = dL_{31}^2/dt = dL_{12}^2/dt = 0$ is satisfied if $L_{12} = L_{23} = L_{31}$ or $A = 0$. If $L_{12} = L_{23} = L_{31}$ then $dA/dt = 0$. Thus equilateral triangles are equilibria. On the other hand, for $A = 0$, we can show that $dA/dt \neq 0$ as follows. Since the collinear configurations correspond to $A = 0$, the ratio between L_{23} and L_{31} satisfies either $L_{23}^2/L_{31}^2 = k_1$ or k_2 . First we consider the case when $L_{23}^2/L_{31}^2 = k_1 < 1$. Then, it follows from (4.9) that the ratios are given by

$$\left. \begin{aligned} \frac{L_{23}}{L_{31}} &= \sqrt{k_1} \equiv \gamma_1 < 1, & \frac{L_{12}}{L_{31}} &= \sqrt{\frac{\Gamma_1 + k_1\Gamma_2}{\Gamma_1 + \Gamma_2}} \equiv \gamma_2 < 1, \\ \frac{L_{12}}{L_{23}} &= \sqrt{\frac{\Gamma_1 + k_1\Gamma_2}{k_1\Gamma_1 + k_1\Gamma_2}} = \frac{\gamma_2}{\gamma_1} > 1, \end{aligned} \right\} \quad (4.12)$$

which indicate $L_{23} < L_{12} < L_{31}$. Moreover, since the configuration of the three α -point vortices is collinear, we have $L_{12} + L_{23} = L_{31}$ and thus $\gamma_1 + \gamma_2 = 1$. Since k_1 is the solution of $f(k_1) = 0$, the constants γ_1 and γ_2 are explicitly represented by

$$\gamma_1 = \frac{1}{\Gamma_1}(\Gamma_1 + \Gamma_2 - \sqrt{\mathcal{R}}), \quad \gamma_2 = 1 - \gamma_1 = \frac{1}{\Gamma_1}(\sqrt{\mathcal{R}} - \Gamma_2), \quad (4.13)$$

in which $\mathcal{R} = \Gamma_1^2 + \Gamma_1\Gamma_2 + \Gamma_2^2$. Then we have $r = L_{31} = L_{12} + L_{23}$, $r - L_{12} = L_{23}$, $r - L_{23} = L_{12}$ and $r - L_{31} = 0$. Substituting these relations into (4.8), we have

$$\begin{aligned} \frac{dA}{dt} &= \frac{1}{4\pi} L_{31} L_{23} L_{31} \sum \Gamma_i L_{23}^{-1} [L_{31}^{-2} B_K(L_{31}) - L_{12}^{-2} B_K(L_{12})] \\ &\quad - \frac{1}{2\pi} L_{31} L_{23} L_{31} \Gamma_2 L_{31}^{-1} [L_{12}^{-2} B_K(L_{12}) - L_{23}^{-2} B_K(L_{23})] \\ &= \frac{1}{4\pi} \left[\Gamma_1 \left(\frac{L_{12}}{L_{31}} B_K(L_{31}) - \frac{L_{31}}{L_{12}} B_K(L_{12}) \right) + \Gamma_2 \left(\frac{L_{12}}{L_{23}} B_K(L_{23}) - \frac{L_{23}}{L_{12}} B_K(L_{12}) \right) \right. \\ &\quad \left. + \Gamma_3 \left(\frac{L_{31}}{L_{23}} B_K(L_{23}) - \frac{L_{23}}{L_{31}} B_K(L_{31}) \right) \right] \\ &= \frac{1}{4\pi} \left[\Gamma_1 \left(\gamma_2 B_K(L_{31}) - \frac{1}{\gamma_2} B_K(\gamma_2 L_{31}) \right) + \Gamma_2 \left(\frac{\gamma_2}{\gamma_1} B_K(\gamma_1 L_{31}) - \frac{\gamma_1}{\gamma_2} B_K(\gamma_2 L_{31}) \right) \right. \\ &\quad \left. - \frac{\Gamma_1 \Gamma_2}{\Gamma_1 + \Gamma_2} \left(\frac{1}{\gamma_1} B_K(\gamma_1 L_{31}) - \gamma_1 B_K(L_{31}) \right) \right] \\ &= \frac{1}{4\pi} \left[\frac{\Gamma_1 \sqrt{\mathcal{R}}}{\Gamma_1 + \Gamma_2} (B_K(L_{31}) - B_K(\gamma_2 L_{31})) + \frac{\Gamma_2 \sqrt{\mathcal{R}}}{\Gamma_1 + \Gamma_2} (B_K(\gamma_1 L_{31}) - B_K(\gamma_2 L_{31})) \right] \\ &\equiv \frac{1}{4\pi} g(L_{31}). \end{aligned} \quad (4.14)$$

We need to confirm that $g(x) \neq 0$ for $x > 0$. Owing to the invariance of (4.3)–(4.5) with respect to the transformation $(\Gamma_1, \Gamma_2, \Gamma_3, t) \mapsto (\Gamma_1/\Gamma_2, 1, \Gamma_3/\Gamma_2, \Gamma_2 t)$, it is sufficient to check it for $\Gamma_1 \geq 1$ and $\Gamma_2 = 1$. The function $g(x)$ is negative for $x > 0$ as

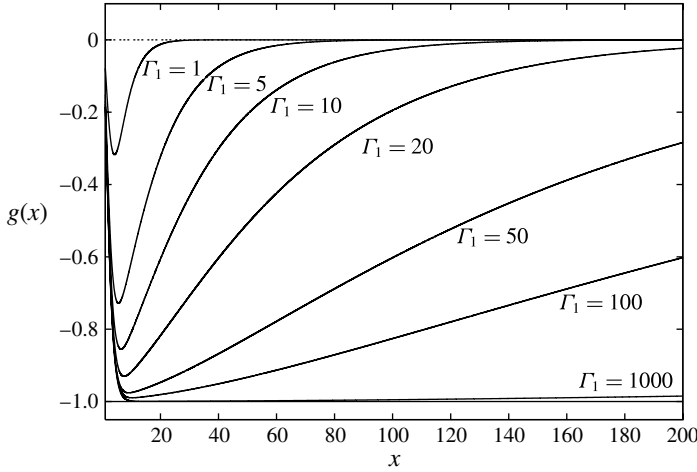


FIGURE 1. Graphs of the function $g(x)$ for various $\Gamma_1 \geq 1$, which show $dA/dt = g(x) < 0$ for $x < 0$.

we see in figure 1. Hence, we have $dA/dt \neq 0$. We can similarly show the same result when the ratio satisfies $L_{23}^2/L_{31}^2 = k_2$. Therefore, the equilibria for the canonical system (4.3)–(4.5) and (4.8) with the conditions (4.1) and (4.2) are equilateral triangles.

Since the canonical system is integrable for $N = 3$, the evolution of the three α -point vortices is described by the contour lines of the Hamiltonian (3.16). As in Newton (2001), with the variables

$$b_1 = \frac{L_{23}^2}{\Gamma_1}, \quad b_2 = \frac{L_{31}^2}{\Gamma_2}, \quad b_3 = \frac{L_{12}^2}{\Gamma_3}, \tag{4.15}$$

each term of the Hamiltonian is expressed by

$$H_0 = -\frac{\Gamma_1 \Gamma_2 \Gamma_3}{4\pi} \left[\frac{1}{\Gamma_1} \log \frac{\Gamma_1 b_1}{\Gamma_3 b_3} + \frac{1}{\Gamma_2} \log \frac{\Gamma_2 b_2}{\Gamma_3 b_3} \right], \tag{4.16}$$

$$H_1 = -\frac{\Gamma_1 \Gamma_2 \Gamma_3}{4\pi} \left[\frac{2}{\Gamma_1} (\mathbf{K}_0(\sqrt{\Gamma_1 b_1}) - \mathbf{K}_0(\sqrt{\Gamma_3 b_3})) + \frac{2}{\Gamma_2} (\mathbf{K}_0(\sqrt{\Gamma_2 b_2}) - \mathbf{K}_0(\sqrt{\Gamma_3 b_3})) \right]. \tag{4.17}$$

The evolution of the three α -point vortices is observed by plotting the contour lines of the Hamiltonian in the two-dimensional (b_1, b_2) -plane, since we have $b_1 + b_2 + b_3 = 0$ owing to (4.2). The wedge-shaped region, $k_1 \leq L_{23}^2/L_{31}^2 = \Gamma_1 b_1/\Gamma_2 b_2 \leq k_2$, is called *the physical region*. Each point on the boundary of the physical region corresponds to a collinear configuration, while those on the continuous line $\Gamma_1 b_1/\Gamma_2 b_2 = 1$ are equilateral triangles, which are equilibria. There are no equilibria in the region $k_1 \leq \Gamma_1 b_1/\Gamma_2 b_2 < 1$ and $1 < \Gamma_1 b_1/\Gamma_2 b_2 \leq k_2$. Figure 2 shows the contour plots of the Hamiltonian for (a) $\Gamma_1 = 1$ and (b) $\Gamma_1 = 2$ with $\Gamma_2 = 1$. The only line connecting to the origin is $\Gamma_1 b_1/\Gamma_2 b_2 = 1$ that represents the equilateral triangles $\Gamma_1 b_1 = \Gamma_2 b_2 = \Gamma_3 b_3$. Since a point in the physical region represents two configurations of the three α -point vortices with opposite arrangements σ_{123} , say $(L_{12}, L_{23}, L_{31}, A)$ and $(L_{12}, L_{23}, L_{31}, -A)$, the physical region can be regarded as two-sided. That is to say, the configurations of $A > 0$ are on the front side, while those of $A < 0$ are on the back side. The two

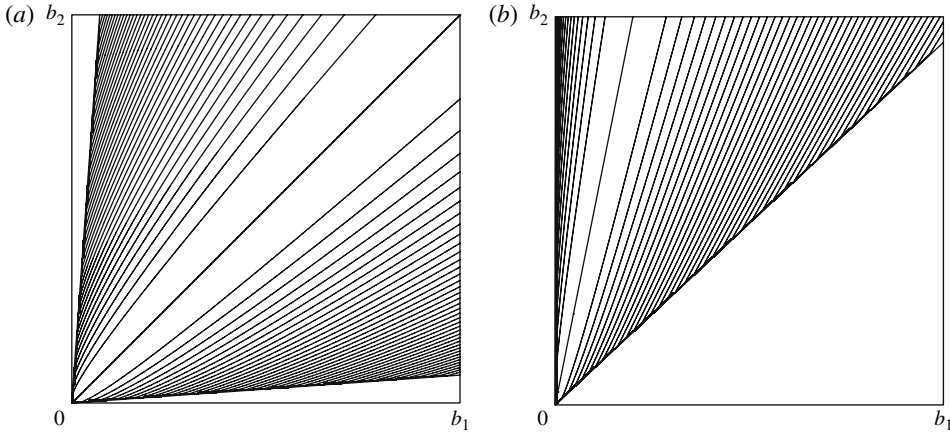


FIGURE 2. Contour plots of the Hamiltonian in the (b_1, b_2) -plane for (a) $\Gamma_1 = 1$ and (b) $\Gamma_1 = 2$. The strength $\Gamma_2 = 1$ can be fixed owing to the temporal scale invariance of the system with respect to $t \mapsto \Gamma_2 t$.

sides are connected at the boundary of the physical region. Therefore, the evolution of the α -point vortices moving along a contour line on one side of the physical region reaches the boundary, at which their configuration becomes collinear, and then it moves back along the same contour line on the other side. Since all contour lines in figure 2 are joined at the boundary of the physical region, we may choose the collinear configuration as initial data, i.e. $A(0) = 0$, without loss of generality. Then we can show that $L_{mn}(t) = L_{mn}(-t)$ and $A(t) = -A(-t)$ for $t \geq 0$ as follows. Suppose that $L_{mn}(t) = L_{mn}(-t)$ and $A(t) = -A(-t)$, then we have

$$\frac{d}{dt}(L_{mn}^2(t) - L_{mn}^2(-t)) = \frac{2}{\pi} \Gamma_k (A(t) + A(-t)) \left[\frac{1}{L_{nk}^2} B_K(L_{nk}) - \frac{1}{L_{km}^2} B_K(L_{km}) \right] = 0, \quad (4.18)$$

$$\frac{d}{dt}(A(t) + A(-t)) = 0, \quad (4.19)$$

which proves the claim because $A(0) = 0$.

The above observations indicate that the evolution of the three α -point vortices as $t \rightarrow \pm\infty$ is characterized by the behaviour of the contour lines of the Hamiltonian as $b_1 \rightarrow \infty$, which is described here. Let us first note that $b_2 \neq 0$ owing to $b_1 \neq 0$. Then we show that $b_2 \rightarrow \infty$ as $b_1 \rightarrow \infty$. Suppose that $b_2 \rightarrow b < \infty$, then it follows from $b_1 + b_2 + b_3 = 0$ that $b_3 \rightarrow -\infty$. While the second term H_1 of the Hamiltonian remains bounded, it follows from

$$\Gamma_3 b_3 = \frac{\Gamma_1 \Gamma_2}{\Gamma_1 + \Gamma_2} (b_1 + b_2) \quad (4.20)$$

that the first term H_0 becomes

$$H_0 = -\frac{\Gamma_1 \Gamma_2 \Gamma_3}{4\pi} \left[\frac{1}{\Gamma_1} \log \frac{\Gamma_1 + \Gamma_2}{\Gamma_2(1 + b_2/b_1)} + \frac{1}{\Gamma_2} \log \frac{(\Gamma_1 + \Gamma_2)b_2/b_1}{\Gamma_1(1 + b_2/b_1)} \right] \rightarrow \infty, \quad (4.21)$$

as $b_1 \rightarrow \infty$ and $b_2 \rightarrow b < \infty$. This contradicts the conservation of the Hamiltonian. Thus we have $b_2 \rightarrow \infty$. Next we assume that $b_2/b_1 \rightarrow \infty$ as $b_1 \rightarrow \infty$. Then the first

term in (4.21) tends to $-\infty$, which is again a contradiction. Consequently, b_2/b_1 converges to a finite non-zero constant, which means that the contour lines of the Hamiltonian approach the line $L_{23}^2/L_{31}^2 = \Gamma_1 b_1/\Gamma_2 b_2 = \text{const.}$ asymptotically as $b_1, b_2 \rightarrow \infty$. Hence, the evolution of the α -point vortices acquires self-similarity as $t \rightarrow \pm\infty$. At the same time, since $b_1 \rightarrow \infty$ and $b_2 \rightarrow \infty$ yield $L_{mn} \rightarrow \infty$, equations (4.3)–(4.5) tend to those for the point-vortex system (2.6) owing to $B_K(x) \rightarrow 1$ as $x \rightarrow \infty$. Moreover, the second term H_1 tends to zero owing to $K_0(x) \rightarrow 0$ as $x \rightarrow \infty$. Thus we have the convergence of the first term

$$\lim_{t \rightarrow \pm\infty} H_0(L_{mn}(t)) = H. \quad (4.22)$$

Therefore, as $t \rightarrow \pm\infty$, the evolution of the three α -point vortices converges asymptotically to the self-similar triple expansion of the three point vortices described in § 2. In other words, owing to (2.21) and $L_{mn}(t) = L_{mn}(-t)$, there exists a constant $C_\infty > 0$ such that the distance $L_{mn}(t)$ converges asymptotically as

$$L_{mn}(t) \rightarrow C_\infty \sqrt{|t|}, \quad t \rightarrow \pm\infty. \quad (4.23)$$

Finally we show a numerical solution of (3.14) to confirm the theoretical results. We choose an initial collinear configuration satisfying $L_{23}/L_{31} = \gamma_1$ and $L_{31} = L_{23} + L_{12}$, which is given by

$$\left. \begin{aligned} (X_1(0), Y_1(0)) &= (-0.5, 0.0), & (X_2(0), Y_2(0)) &= (0.5 - \gamma_1, 0.0), \\ (X_3(0), Y_3(0)) &= (0.5, 0.0). \end{aligned} \right\} \quad (4.24)$$

As the numerical scheme, we use an implicit fourth-order symplectic Runge–Kutta method (Leimkuhler & Reich 2005) with the time step size $\Delta t = 0.001$, since we need an accurate numerical solution for longer time to investigate the behaviour of the solution as $\alpha \rightarrow 0$ in the next section. Thanks to the symplectic scheme, the maximum error of the Hamiltonian is less than 1.0×10^{-12} up to the time $t = 10^5$, which is tolerable. The solution in the negative time direction is recovered according to $L_{mn}(t) = L_{mn}(-t)$ and $A(t) = -A(-t)$.

Figure 3 shows the orbits of the three α -point vortices from $t = 0$ to $t = 900$. Starting from the collinear configuration, the α -point vortices rotate in the counterclockwise direction with increasing relative distances. The evolution of the distances $L_{mn}(t)$ between the α -point vortices for $t > 0$ is shown in figure 4(a), which indicates that they grow asymptotically as \sqrt{t} for large t . On the other hand, figure 4(b) shows that the evolution of the ratios $L_{23}/L_{31}(t)$ and $L_{12}/L_{31}(t)$ is almost constant for large $|t|$, which means that the evolution of the α -point vortices acquires self-similarity. The ratios change greatly for small $|t|$ and have their minima at $t = 0$ when the α -point vortices reach the collinear configuration. Hence, the numerical solution demonstrates that the three α -point vortices approach asymptotically the self-similar triple expansion as $t \rightarrow \pm\infty$.

4.2. Instantaneous energy and enstrophy variations via triple collapse

With the evolution of the three α -point vortices given in the previous section, we observe how the Hamiltonian energy, the energy $E^{(\alpha)}$ and the enstrophy $\mathcal{E}^{(\alpha)}$ converge as α tends to zero. The $\alpha \rightarrow 0$ limit of the evolution of the three α -point vortices is derived with the scaling property (3.15). Let us note that for fixed $t \neq 0$, $|t|/\alpha^2 \rightarrow \infty$

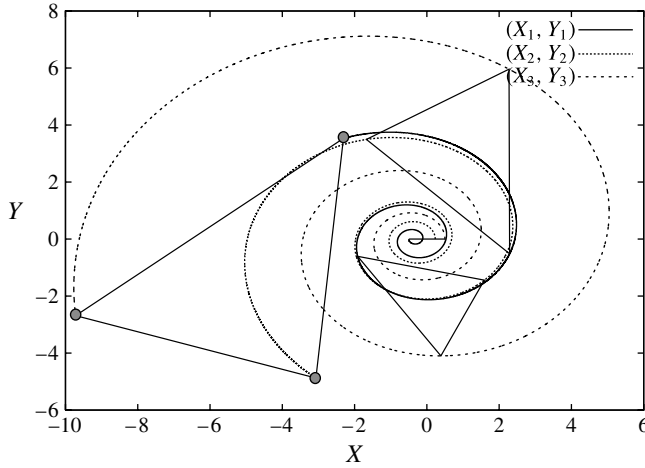


FIGURE 3. Orbits of the three α -point vortices from $t = 0$ to 900 starting from the collinear initial configuration (4.24).

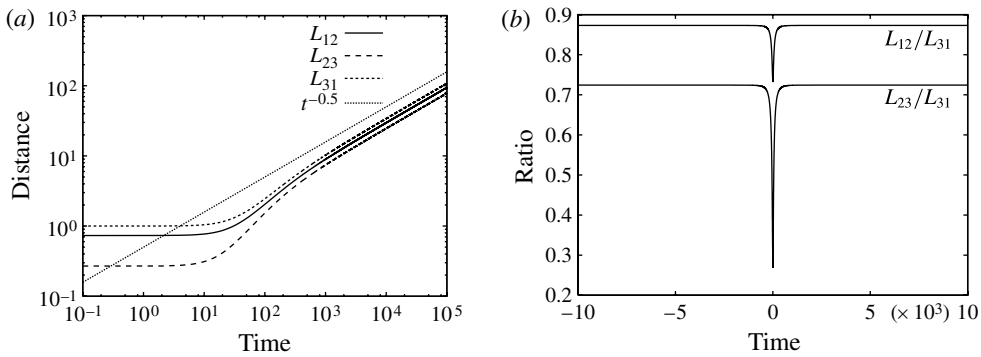


FIGURE 4. (a) Log-log plot of the evolution of the distances $L_{12}(t)$, $L_{23}(t)$ and $L_{31}(t)$ between the three α -point vortices for $0 < t \leq 10\,000$. (b) Evolution of their ratios $L_{23}/L_{31}(t)$ and $L_{12}/L_{31}(t)$ for $-10\,000 \leq t \leq 10\,000$.

as $\alpha \rightarrow 0$. Then it follows from the asymptotic behaviour (4.23) that we have

$$l_{mn}(t) = \alpha L_{mn} \left(\frac{t}{\alpha^2} \right) \longrightarrow C_\infty \alpha \frac{\sqrt{|t|}}{\alpha} = C_\infty \sqrt{|t|}, \quad \alpha \rightarrow 0, \quad (4.25)$$

which indicates that the evolution of the three α -point vortices tends to the self-similar triple collapse for $t < 0$ and the self-similar triple expansion for $t > 0$. The convergence is clearly observed in figure 5, in which log-log plots of $\alpha L_{31}(t/\alpha^2)$ for various α are shown for (a) $\Gamma_1 = 1$ and $\Gamma_2 = 1$ and (b) $\Gamma_1 = 5$ and $\Gamma_2 = 1$.

In the point-vortex system, the energy E_p is equivalent to the Hamiltonian energy H_p , but the energy $E^{(\alpha)}$ is different from the Hamiltonian energy for the α PV system. Thus we need to consider the convergence of the two energies for $\alpha \rightarrow 0$ separately. The Hamiltonian energy H_p of the point-vortex system is no longer a conserved quantity for the α PV system, but it is computed from the solution of the canonical system

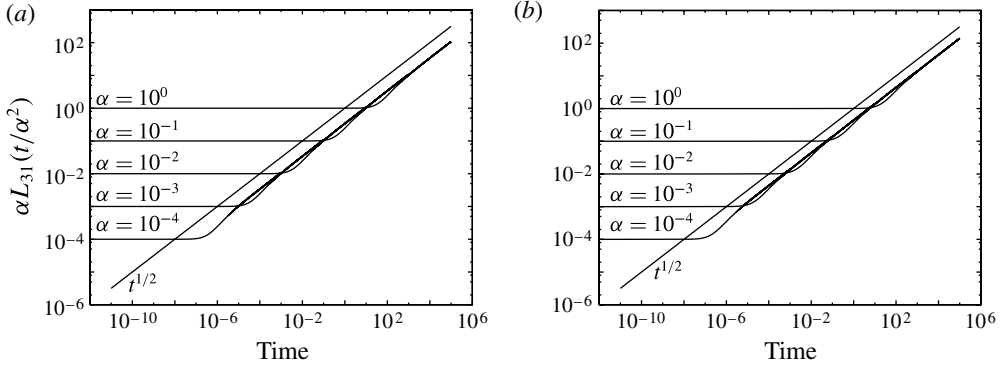


FIGURE 5. Log–log plots of $\alpha L_{31}(t/\alpha^2)$ for various α ; (a) $\Gamma_1 = 1$ and $\Gamma_2 = 1$ and (b) $\Gamma_1 = 5$ and $\Gamma_2 = 1$, which show the convergence to \sqrt{t} as $\alpha \rightarrow 0$.

with (3.16) and (4.1):

$$\begin{aligned}
 H_p^{(\alpha)}(t) &= -\frac{1}{2\pi} \sum_{m=1}^3 \sum_{n=m+1}^3 \Gamma_m \Gamma_n \log l_{mn}(t) = -\frac{1}{2\pi} \sum_{m=1}^3 \sum_{n=m+1}^3 \Gamma_m \Gamma_n \log \alpha L_{mn} \left(\frac{t}{\alpha^2} \right) \\
 &= -\frac{1}{2\pi} \sum_{m=1}^3 \sum_{n=m+1}^3 \Gamma_m \Gamma_n \log L_{mn} \left(\frac{t}{\alpha^2} \right) = H_0 \left(\frac{t}{\alpha^2} \right) = H - H_1 \left(\frac{t}{\alpha^2} \right) \\
 &= H + \frac{1}{2\pi} \sum_{m=1}^3 \sum_{n=m+1}^3 \Gamma_m \Gamma_n \mathbf{K}_0 \left(L_{mn} \left(\frac{t}{\alpha^2} \right) \right). \tag{4.26}
 \end{aligned}$$

For $t \neq 0$, since $L_{mn}(t/\alpha^2) \rightarrow \infty$ as $\alpha \rightarrow 0$, we have $H_1(t/\alpha^2) \rightarrow 0$. Thus we have the convergence of the Hamiltonian energy:

$$\lim_{\alpha \rightarrow 0} H_p^{(\alpha)}(t) \longrightarrow H \quad \text{for } t \neq 0. \tag{4.27}$$

On the other hand, it follows from $H_p^{(\alpha)}(\alpha^2 t) = H - H_1(t)$ that $H_p^{(\alpha)}(\alpha^2 t)$ for any t converges to $H_p^{(\alpha)}(0)$. Hence, it is localized in the neighbourhood of $t = 0$ as α tends to zero. Because of the localization, the variation of the Hamiltonian energy at $t = 0$ is defined by

$$\lim_{\alpha \rightarrow 0} H_p^{(\alpha)}(0) - H = \frac{1}{2\pi} \sum_{m=1}^3 \sum_{n=m+1}^3 \Gamma_m \Gamma_n \mathbf{K}_0(L_{mn}(0)) = -H_1(0). \tag{4.28}$$

Figure 6(a) shows the evolution of $H_p^{(\alpha)}(t)$ for various α computed from the numerical solution for $\Gamma_1 = \Gamma_2 = 1$. This indicates that, in the limit of $\alpha \rightarrow 0$, the Hamiltonian energy is conserved during the triple collapse for $t < 0$ and the triple expansion for $t > 0$, while it jumps instantly at the critical time $t = 0$. The magnitude of the energy variation $H_1(0)$ is determined by the initial collinear configuration. Figure 7(a) shows log plots of $H_1(0)$ for the collinear configurations along the boundary of the physical region when $\Gamma_1 = \Gamma_2 = 1$. Since they are positive, the Hamiltonian energy always jumps discontinuously in the negative direction at the critical time.

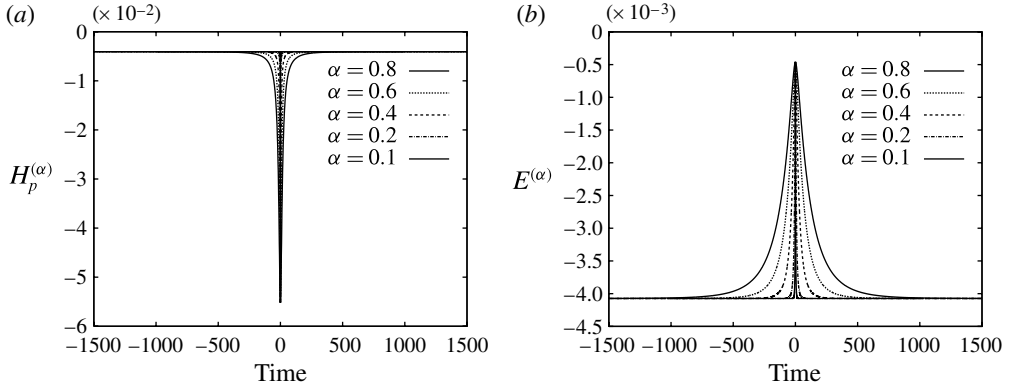


FIGURE 6. Evolution of (a) the Hamiltonian energy $H_p^{(\alpha)}(t)$ and (b) the energy $E^{(\alpha)}(t)$ for various α . The vortex strengths are $\Gamma_1 = \Gamma_2 = 1$. As α tends to zero, they are localized in the neighbourhood of $t = 0$, whereas they converge to the same constant for $t \neq 0$. They illustrate that the Hamiltonian energy and the energy jump discontinuously at time $t = 0$ in the limit.

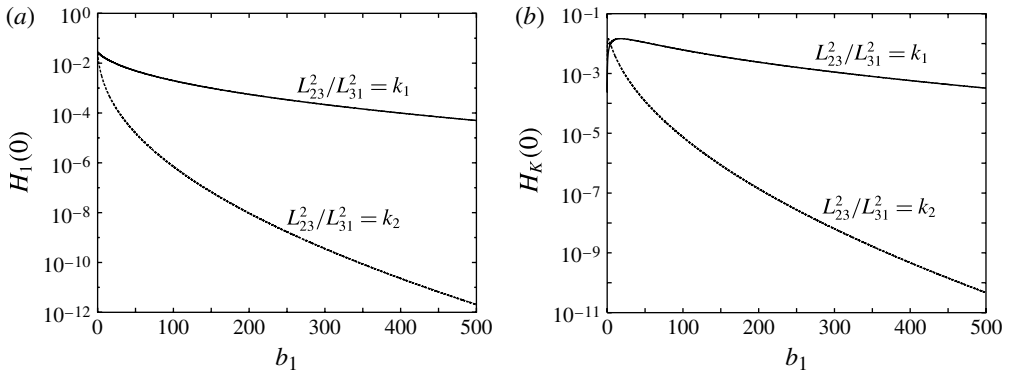


FIGURE 7. (a) Log plot of $H_1(0)$ for the collinear initial configurations along the boundary of the physical region, $L_{23}^2/L_{31}^2 = \Gamma_1 b_1/\Gamma_2 b_2 = k_1$ and k_2 . (b) Log plot of $H_K(0)$ for the collinear configurations. The vortex strengths are $\Gamma_1 = 1$ and $\Gamma_2 = 1$.

The energy $E^{(\alpha)}$ is computed from the distance $L_{mn}(t)$ as follows:

$$\begin{aligned}
 E^{(\alpha)}(\alpha^2 t) &= -\frac{1}{2\pi} \sum_{m=1}^3 \sum_{n=m+1}^3 \Gamma_m \Gamma_n \left[\log \frac{l_{mn}(\alpha^2 t)}{\alpha} + \mathbf{K}_0 \left(\frac{l_{mn}(\alpha^2 t)}{\alpha} \right) \right. \\
 &\quad \left. + \frac{l_{mn}(\alpha^2 t)}{2\alpha} \mathbf{K}_1 \left(\frac{l_{mn}(\alpha^2 t)}{\alpha} \right) \right] \\
 &= -\frac{1}{2\pi} \sum_{m=1}^3 \sum_{n=m+1}^3 \Gamma_m \Gamma_n \left[\log L_{mn}(t) + \mathbf{K}_0(L_{mn}(t)) + \frac{1}{2} L_{mn}(t) \mathbf{K}_1(L_{mn}(t)) \right] \\
 &= H - \frac{1}{4\pi} \sum_{m=1}^3 \sum_{n=m+1}^3 \Gamma_m \Gamma_n L_{mn}(t) \mathbf{K}_1(L_{mn}(t)). \tag{4.29}
 \end{aligned}$$

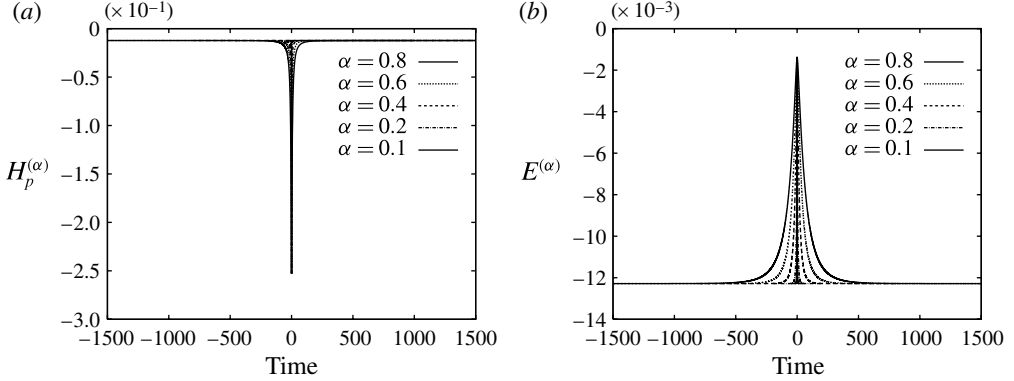


FIGURE 8. Evolution of (a) the Hamiltonian energy $H_p^{(\alpha)}(t)$ and (b) $E^{(\alpha)}(t)$ for various α . The vortex strengths are $\Gamma_1 = 5$ and $\Gamma_2 = 1$. The Hamiltonian energy and the energy jump discontinuously at the critical time $t = 0$ in the limit.

Hence, we have for $\tau = \alpha^2 t$

$$E^{(\alpha)}(\tau) = H - \frac{1}{4\pi} \sum_{m=1}^3 \sum_{n=m+1}^3 \Gamma_m \Gamma_n L_{mn} \left(\frac{\tau}{\alpha^2} \right) \mathbf{K}_1 \left(L_{mn} \left(\frac{\tau}{\alpha^2} \right) \right) \equiv H + H_K \left(\frac{\tau}{\alpha^2} \right). \quad (4.30)$$

The energy $E^{(\alpha)}(\tau)$ is localized at $\tau = 0$ in a similar manner to the Hamiltonian energy, the variation of which is defined by

$$\lim_{\alpha \rightarrow 0} E^{(\alpha)}(0) - H = -\frac{1}{4\pi} \sum_{m=1}^3 \sum_{n=m+1}^3 \Gamma_m \Gamma_n L_{mn}(0) \mathbf{K}_1(L_{mn}(0)) = H_K(0). \quad (4.31)$$

The evolution of $E^{(\alpha)}(\tau)$ for various α with $\Gamma_1 = \Gamma_2 = 1$ is shown in figure 6(b), which clearly demonstrates the instantaneous finite energy surge at the critical time. This phenomenon occurs because the filtering effect of the α -regularization gets stronger as the α -point vortices tend to collapse, i.e. when they become infinitely close. The energy variation $H_K(0)$ is also computed from the initial collinear configuration, which is always positive for the collinear configurations along the boundary of the physical region as shown in figure 7(b). The discontinuous jumps in the Hamiltonian energy and the energy $E^{(\alpha)}$ variations at the critical time are also observed for the other vortex strengths. See figure 8 for $\Gamma_1 = 5$ and $\Gamma_2 = 1$.

The energy dissipation rate $\mathcal{D}_E^{(\alpha)}(\tau)$ is obtained by differentiating (4.30):

$$\begin{aligned} \mathcal{D}_E^{(\alpha)}(\tau) &= -\frac{1}{4\pi\alpha^2} \sum_{m=1}^3 \sum_{n=m+1}^3 \Gamma_m \Gamma_n \frac{dL_{mn}}{d\tau} \left(\frac{\tau}{\alpha^2} \right) \\ &\quad \times \left[\mathbf{K}_1 \left(L_{mn} \left(\frac{\tau}{\alpha^2} \right) \right) + L_{mn} \left(\frac{\tau}{\alpha^2} \right) \frac{d}{dx} \mathbf{K}_1 \left(L_{mn} \left(\frac{\tau}{\alpha^2} \right) \right) \right] \\ &= \frac{1}{4\pi\alpha^2} \sum_{m=1}^3 \sum_{n=m+1}^3 \Gamma_m \Gamma_n \frac{dL_{mn}}{d\tau} \left(\frac{\tau}{\alpha^2} \right) L_{mn} \left(\frac{\tau}{\alpha^2} \right) \mathbf{K}_0 \left(L_{mn} \left(\frac{\tau}{\alpha^2} \right) \right) \\ &\equiv \frac{1}{\alpha^2} F \left(\frac{\tau}{\alpha^2} \right), \end{aligned} \quad (4.32)$$

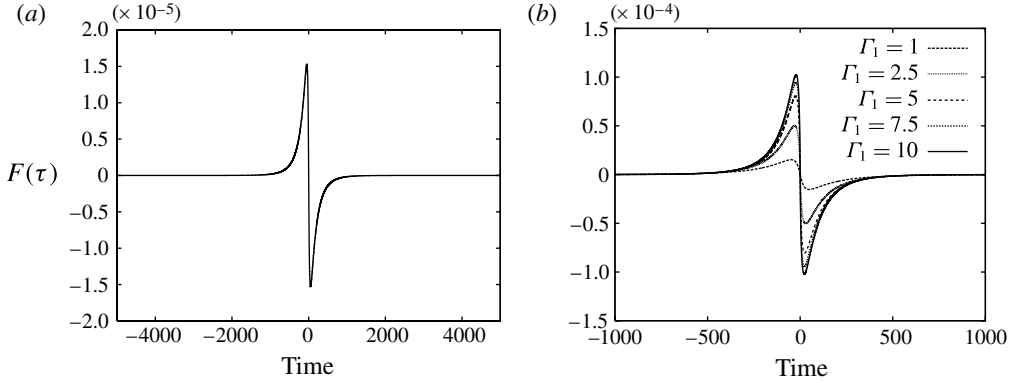


FIGURE 9. (a) The function $F(\tau)$ computed from the numerical solution for $\Gamma_1 = 1$ and $\Gamma_2 = 1$. (b) Plots of $F(\tau)$ for various $\Gamma_1 = 1, 2.5, 5, 7.5$ and 10 and $\Gamma_2 = 1$.

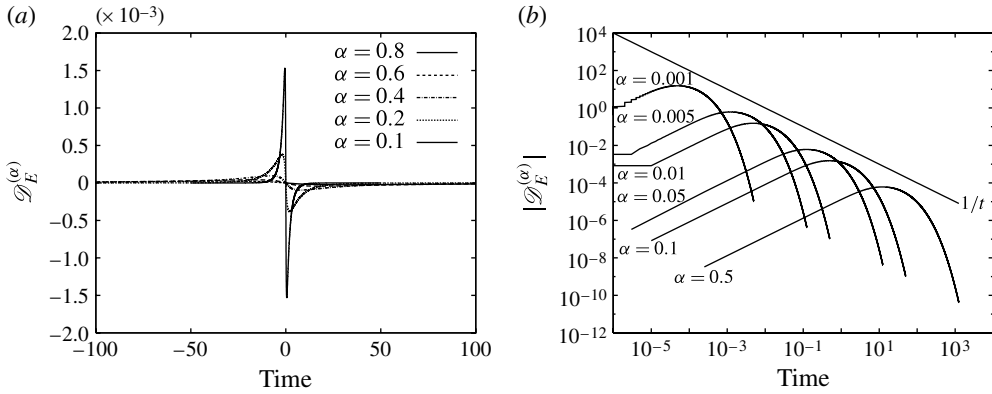


FIGURE 10. (a) Convergence of the energy dissipation rate $\mathcal{D}_E^{(\alpha)}(t)$ for $t \in [-100, 100]$ for various α . (b) Log-log plot of $|\mathcal{D}_E^{(\alpha)}(t)|$ for $t > 0$.

in which the function $F(\tau)$ is defined by

$$F(\tau) = \frac{1}{4\pi} \sum_{m=1}^3 \sum_{n=m+1}^3 \Gamma_m \Gamma_n \frac{dL_{mn}}{d\tau}(\tau) L_{mn}(\tau) K_0(L_{mn}(\tau)). \quad (4.33)$$

Figure 9(a) shows the graph of the function $F(\tau)$ computed from the numerical solution for $\Gamma_1 = \Gamma_2 = 1$. As we observe in figure 9(b), this profile of the function $F(\tau)$ is similar to those for the other values of $\Gamma_1 = 2.5, 5, 7.5$ and 10 with fixed $\Gamma_2 = 1$. The convergence of the energy dissipation rate for the case $\Gamma_1 = \Gamma_2 = 1$ is shown in figure 10(a). For $\tau \neq 0$, the dissipation rate converges to zero as $\alpha \rightarrow 0$, while it is localized in the neighbourhood of $\tau = 0$ and its maximum and minimum diverge as $\alpha \rightarrow 0$. In order to see the convergence more closely, we show a log-log plot of the energy dissipation rate for $\tau > 0$ in figure 10(b), which indicates that the energy dissipation rate is localized in the neighbourhood of $\tau = 0$ with keeping the profile of the function $F(\tau)$ unchanged, and its maximum diverges like $1/\tau$. The limit

of the energy dissipation rate is no longer a function, since it diverges at $\tau = 0$. In fact, we can show the convergence to the zero energy dissipation rate in the sense of distributions regardless of the vortex strengths as follows. Since the function $F(\tau)$ is odd, namely $F(\tau) + F(-\tau) = 0$ as we see in figure 9, we have, for any compactly supported smooth function $\varphi(\tau)$,

$$\begin{aligned} \langle D_E^{(\alpha)}, \varphi \rangle &= \int_{-\infty}^{\infty} \frac{1}{\alpha^2} F\left(\frac{\tau}{\alpha^2}\right) \varphi(\tau) \, d\tau \\ &= \int_{-\infty}^{\infty} F(s) \varphi(\alpha^2 s) \, ds \longrightarrow \varphi(0) \int_{-\infty}^{\infty} F(s) \, ds = 0, \end{aligned} \tag{4.34}$$

as $\alpha \rightarrow 0$. Hence we have

$$\lim_{\alpha \rightarrow 0} \mathcal{D}_E^{(\alpha)} = 0, \tag{4.35}$$

in the sense of distributions. This does not contradict the existence of the discontinuous jump in the energy $E^{(\alpha)}$ variation, since the magnitude of the jump at the critical time is finite, which is negligible in the distributional sense.

In the rest of this section, we examine the enstrophy variation. Owing to (3.15), the non-constant part of the enstrophy (3.12) is rewritten by

$$\mathcal{Z}^{(\alpha)}(\alpha^2 t) = \frac{1}{4\pi\alpha^2} \sum_{m=1}^3 \sum_{n=m+1}^3 \Gamma_n \Gamma_m L_{mn}(t) \mathbf{K}_1(L_{mn}(t)). \tag{4.36}$$

Hence, for $\tau = \alpha^2 t$, we have

$$\mathcal{Z}^{(\alpha)}(\tau) = \frac{1}{4\pi\alpha^2} \sum_{m=1}^3 \sum_{n=m+1}^3 \Gamma_n \Gamma_m L_{mn}\left(\frac{\tau}{\alpha^2}\right) \mathbf{K}_1\left(L_{mn}\left(\frac{\tau}{\alpha^2}\right)\right) = -\frac{1}{\alpha^2} H_K\left(\frac{\tau}{\alpha^2}\right). \tag{4.37}$$

Note that $H_K(\tau)$ is the same function that represents the magnitude of the energy variation in (4.30). The limit of $\mathcal{Z}^{(\alpha)}(\tau)$ is no longer a function, since it tends to zero for $\tau \neq 0$, while it diverges at $\tau = 0$. Thus we consider the convergence of $\mathcal{Z}^{(\alpha)}$ in the sense of distributions. For any compactly supported smooth function $\varphi(\tau)$, we have

$$\begin{aligned} \langle \mathcal{Z}^{(\alpha)}, \varphi \rangle &= - \int_{-\infty}^{\infty} \frac{1}{\alpha^2} H_K\left(\frac{\tau}{\alpha^2}\right) \varphi(\tau) \, d\tau \\ &= - \int_{-\infty}^{\infty} H_K(s) \varphi(\alpha^2 s) \, ds \longrightarrow -z_0 \varphi(0), \end{aligned} \tag{4.38}$$

as $\alpha \rightarrow 0$, where

$$z_0 = \int_{-\infty}^{\infty} H_K(s) \, ds. \tag{4.39}$$

Hence, we have

$$\lim_{\alpha \rightarrow 0} \mathcal{Z}^{(\alpha)} = -z_0 \delta, \tag{4.40}$$

in the sense of distributions. Note that z_0 is positive and finite, since the function $H_K(t)$ is always positive and rapidly decreasing as we see in figure 11. Consequently, the limit of the enstrophy variation is the δ measure with the negative mass of $-z_0$. In other words, it follows from (4.40) that we have the convergence of the total enstrophy

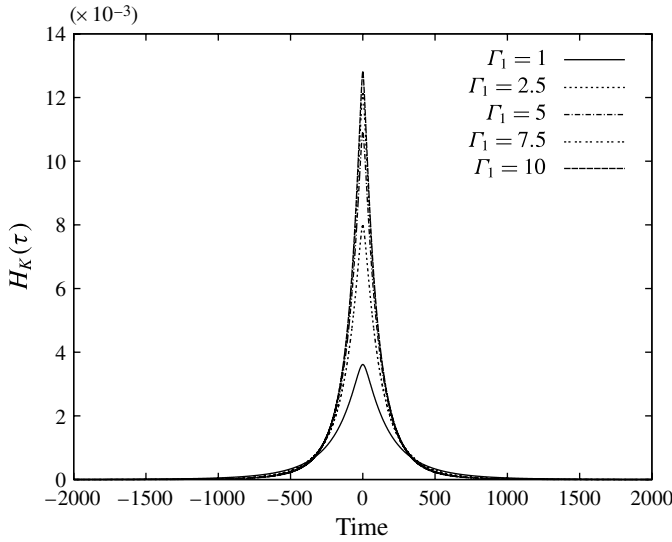


FIGURE 11. Plots of the function $H_K(\tau)$ computed from the numerical solution for various $\Gamma_1 = 1, 2.5, 5, 7.5$ and 10 and $\Gamma_2 = 1$.

variation,

$$\int_{-\infty}^T \mathcal{L}^{(\alpha)}(\tau) d\tau \rightarrow -z_0 \mathcal{H}(T), \tag{4.41}$$

in which $\mathcal{H}(T)$ represents the Heaviside function. Hence, the total variation of the enstrophy is zero until the collapsing time $T = 0$ and it drops to $-z_0$ beyond the critical time, which indicates that the enstrophy *dissipates* via the self-similar triple collapse.

4.3. Robustness of the enstrophy dissipation via the self-similar triple collapse

In order to examine whether the singular self-similar orbit with the enstrophy dissipation is obtained without the conditions (4.1) and (4.2), we examine the numerical evolution of the three α -point vortices when the condition (4.2) is not satisfied. That is to say, we solve the canonical equation (3.14) numerically with the following conditions:

$$\frac{1}{\Gamma_1} + \frac{1}{\Gamma_2} + \frac{1}{\Gamma_3} = 0, \quad M = \Gamma_1 \Gamma_2 L_{12}^2 + \Gamma_2 \Gamma_3 L_{23}^2 + \Gamma_3 \Gamma_1 L_{31}^2 = \varepsilon_M \neq 0. \tag{4.42}$$

The vortex strengths are $\Gamma_1 = \Gamma_2 = 1$. The isosceles configuration of the three α -point vortices satisfying $M = \varepsilon_M$ and $L_{23}(0) = L_{31}(0) = 1$ is chosen as the initial data. Figure 12(a) shows the evolution of the distances $L_{12}(t)$, $L_{23}(t)$ and $L_{31}(t)$ for $\varepsilon_M = 0.03$, which indicates that the distances behave asymptotically as \sqrt{t} for $t \rightarrow \infty$. Similarly, we can also confirm that they grow asymptotically like $\sqrt{|t|}$ for $t \rightarrow -\infty$. On the other hand, the evolution of the ratios $L_{23}/L_{31}(t)$ and $L_{12}/L_{31}(t)$ for $\varepsilon_M = 0.03$ is plotted in figure 12(b), which shows that the ratios tend to some constants for $t \rightarrow \pm\infty$. Therefore, with the same argument as in §4.2, the evolution of the three α -point vortices converges to the self-similar triple collapse for $t < 0$ and to the self-similar triple expansion for $t > 0$ as $\alpha \rightarrow 0$. Let us note that the

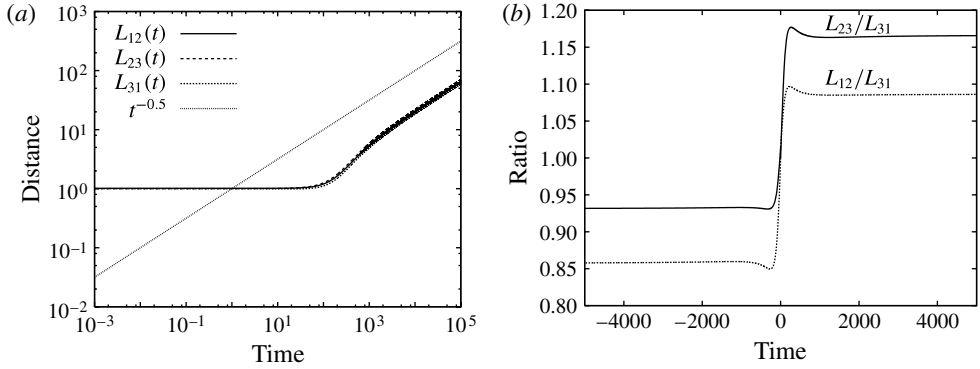


FIGURE 12. (a) Log–log plot of the evolution of $L_{12}(t)$, $L_{23}(t)$ and $L_{31}(t)$ for $t > 0$. (b) Evolution of the ratios $L_{23}/L_{31}(t)$ and $L_{12}/L_{31}(t)$. The magnitude of perturbation is $\varepsilon_M = 0.03$ and the vortex strengths are $\Gamma_1 = \Gamma_2 = 1$.

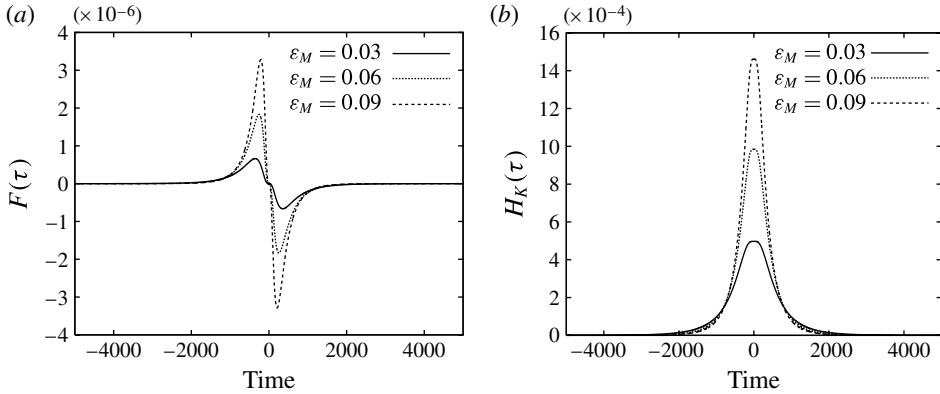


FIGURE 13. Plots of the functions (a) $F(\tau)$ and (b) $H_K(\tau)$ computed from the numerical solutions of the canonical equations for $\varepsilon_M = 0.03, 0.06$ and 0.09 . The vortex strengths are $\Gamma_1 = \Gamma_2 = 1$.

convergence to the singular self-similar orbit is also observed for a range of $\varepsilon_M > 0$. In order to see the variations of the energy dissipation rate and the enstrophy along the singular self-similar orbit, we plot the functions $F(\tau)$ and $H_K(\tau)$ for $\varepsilon_M = 0.03, 0.06$ and 0.09 in figures 13(a) and 13(b) respectively. Since the function $F(\tau)$ is odd, we have $\lim_{\alpha \rightarrow 0} \mathcal{D}_E^{(\alpha)} = 0$ in the sense of distributions. On the other hand, the function $H_K(\tau) > 0$ is even and rapidly decreasing, and thus we have the convergence of the enstrophy variation, $\lim_{\alpha \rightarrow 0} \mathcal{L}^{(\alpha)} = -z_0 \delta$ with some $z_0 > 0$, in the sense of distributions similarly to § 4.2.

The evolution of the three α -point vortices becomes different when ε_M is negative. Figures 14(a) and 14(b) show the evolution of the distances between the α -point vortices and their ratios for $\varepsilon_M = -0.03$ respectively. The vortex strengths and the initial configurations are the same as those considered above. Since the evolution of the three α -point vortices is periodic, there exists a constant C_L such that $|L_{mn}(t)| < C_L$. Hence, it follows from (3.15) that $|l_{mn}(t)| = |\alpha L_{mn}(t/\alpha^2)| \leq C_L |\alpha| \rightarrow 0$ as $\alpha \rightarrow 0$.

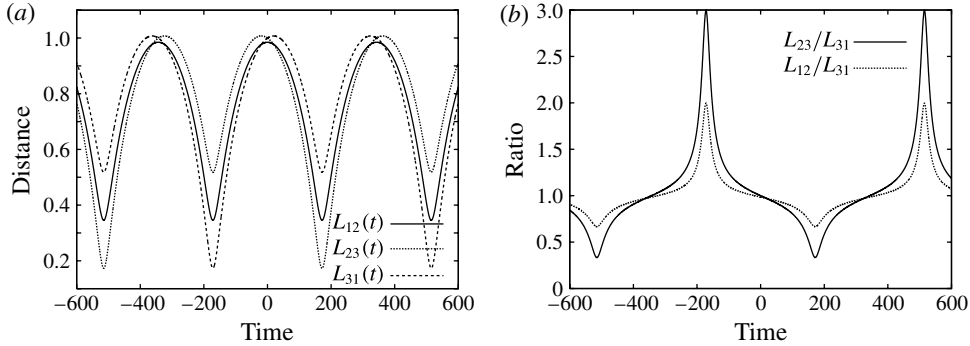


FIGURE 14. (a) Plots of the distances $L_{12}(t)$, $L_{23}(t)$ and $L_{31}(t)$. (b) Evolution of the ratios $L_{23}/L_{31}(t)$ and $L_{12}/L_{31}(t)$. The magnitude of perturbation is $\varepsilon_M = -0.03$. The vortex strength are $\Gamma_1 = \Gamma_2 = 1$.

Hence, the three α -point vortices converge to a point in the limit of $\alpha \rightarrow 0$, which is not the convergence to the singular self-similar orbit. The convergence to a point is observed for $\varepsilon_M < 0$.

These numerical examples illustrate that the convergence to the singular self-similar orbit with the enstrophy dissipation is observed for a certain range of $\varepsilon_M \geq 0$. Hence, neither of the conditions (4.1) and (4.2) is required to obtain the singular self-similar orbit with the enstrophy dissipation. This also suggests a clear difference between the point-vortex system and the $\alpha \rightarrow 0$ limit of the α PV system, since both of the conditions are necessary to obtain the self-similar triple collapse and expansion in the point-vortex system (Newton 2001).

5. Summary and discussion

We have constructed a singular weak solution of the two-dimensional Euler equations by considering the α -point-vortex system, whose evolution corresponds to a unique global weak solution of the two-dimensional Euler- α equations in the sense of distributions. We have obtained some basic results for the α PV system for general N , which are summarized as follows.

- (a) The energy $E^{(\alpha)}(t)$ generated by the evolution of the α -point vortices is represented by (3.9), which is different from the Hamiltonian energy of the α PV system.
- (b) The α PV system (3.3) is reduced to the canonical Hamiltonian dynamical system (3.14) owing to the scaling property (3.15), which enables us to investigate the behaviour of the solution of the α PV system as α tends to zero.
- (c) The α PV system has the same integrability as the point-vortex system. In particular, it is integrable for $N = 3$.

We have then investigated the solution of the canonical equation for the integrable case $N = 3$ subject to the additional conditions (4.1) and (4.2). While these conditions allow the emergence of the self-similar triple collapse in the point-vortex system, no collapse occurs in the α PV system. We prove that the equilateral triangles are the only equilibria. By plotting the contour plots of the Hamiltonian, we show that the evolution of the three α -point vortices for the initial collinear configuration approaches asymptotically the self-similar triple expansion as $t \rightarrow \pm\infty$.

We have finally examined the evolution of the three α -point vortices, the Hamiltonian energy $H_p^{(\alpha)}(t)$, the energy $E^{(\alpha)}(t)$ and the enstrophy $\mathcal{E}^{(\alpha)}(t)$ as $\alpha \rightarrow 0$.

- (a) As $\alpha \rightarrow 0$, the evolution of the three α -point vortices for the collinear initial configuration tends to the triple collapse for $t < 0$ and the triple expansion for $t > 0$, which means that the two singular self-similar evolutions in the point-vortex system are connected at the critical time $t = 0$ as the $\alpha \rightarrow 0$ limit solution of the α PV system.
- (b) In the limit of $\alpha \rightarrow 0$, the Hamiltonian energy $H_p^{(\alpha)}(t)$ and the energy $E^{(\alpha)}(t)$ jump discontinuously at the critical time. The limit of the energy dissipation rate $\mathcal{D}_E^{(\alpha)}(t)$ is no longer a function, but we prove that $\lim_{\alpha \rightarrow 0} \mathcal{D}_E^{(\alpha)} \rightarrow 0$ in the sense of distributions, which indicates that the energy dissipation does not occur via the triple collapse.
- (c) As $\alpha \rightarrow 0$, the enstrophy $\mathcal{E}^{(\alpha)}$ converges to $-z_0\delta$ in the sense of distributions. Since the mass of the δ measure $-z_0$ is negative, the enstrophy dissipates in a sense such that the total enstrophy is reduced by $-z_0$ via the collapse of the three α -point vortices.
- (d) The convergence to the singular self-similar orbit with the enstrophy dissipation is obtained in the limit of $\alpha \rightarrow 0$, even if the conditions (4.1) and (4.2) are not satisfied simultaneously.

The present study indicates that the self-similar triple collapse is a robust mechanism of enstrophy dissipation in the sense that it is observed continuously for a certain range of the parameter region. On the other hand, in spite of its significance, we only consider the evolution of the three α -point vortices and thus we are unable to draw definite conclusions on the relation between the singular self-similar orbit with enstrophy dissipation and two-dimensional turbulence. Hence, further scrutiny of the α PV system is required to understand the relation. In what follows, we address some possible future problems suggested by the present study. The notable features of the singular evolution presented here are the integrability and the self-similarity, but their significance is unclear. Therefore, it would be interesting to examine if the enstrophy dissipation occurs for the self-similar evolution of more than three α -point vortices in the limit of $\alpha \rightarrow 0$. Furthermore, it would be possible to obtain a chaotic solution with enstrophy dissipation when the self-similar orbit is perturbed, since the α PV system for $N \geq 4$ is generally non-integrable as shown in § 3.2. The existence of such a chaotic evolution and its connection with two-dimensional turbulence need to be investigated. Of course, we are unable to rule out the possibility that non-self-similar evolutions of the α PV system dissipate the enstrophy as α tends to zero. Constructing such non-self-similar dissipative evolutions of many α -point vortices is another future problem.

Let us finally make some mathematical remarks. The evolution of the three α -point vortices loses its regularity as $\alpha \rightarrow 0$ in the sense that the enstrophy varies via the self-similar triple collapse. The enstrophy dissipation occurs after an infinitely long time, since we suppose that the three α -point vortices collapse at $t = 0$ and the scaled time $t_c/\alpha^2 \rightarrow -\infty$ as $\alpha \rightarrow 0$ for arbitrary fixed time $t_c < 0$. On the other hand, rigorously speaking, we need to see how the limit singular solution corresponds to a weak solution of the two-dimensional Euler equations mathematically, which gives rise to the following questions: *Suppose that $\mathbf{u}^{(\alpha)}$ be a global weak solution of the Euler- α equations in the space of Radon measure on \mathbb{R}^2 . Then can we regard the limit $\mathbf{u}^{(0)} = \lim_{\alpha \rightarrow 0} \mathbf{u}^{(\alpha)}$ as a weak solution of the two-dimensional Euler equations? If so, in*

what mathematical sense is it justified? These questions have been partially answered by Bardos, Linshiz & Titi (2010). They have shown that the global weak solution for vortex-sheet initial data with fixed sign, which is an example of the vorticity distribution in the space of Radon measure on \mathbb{R}^2 , converges to a vortex-sheet weak solution of the two-dimensional Euler equations as $\alpha \rightarrow 0$. However, considering the convergence for the initial vorticity field of discrete δ -functions is not a straightforward problem, since the two-dimensional Euler- α equations admit a unique global weak solution, whereas the two-dimensional Euler equations have no weak solution for such initial vorticity data.

Acknowledgements

The author would like to thank the referees for their comments. The author also thank Professor H. Nawa, Professor G. Kawahara, Professor M. Yamada and Professor T. Matsumoto for fruitful discussions and comments. The present study is partially supported by JSPS grants nos 21340017 and 23340030.

REFERENCES

- AREF, H. 1979 Motion of three vortices. *Phys. Fluids* **22** (3), 393–400.
- BARDOS, C., LINSHIZ, J. S. & TITI, E. S. 2010 Global regularity and convergence of a Birkhoff–Rott- α approximation of the dynamics of vortex sheets of the two-dimensional Euler equations. *Commun. Pure Appl. Maths* **63**, 697–746.
- BATCHELOR, G. K. 1969 Computation of the energy spectrum in homogeneous two-dimensional turbulence. *Phys. Fluids Suppl. II* **12**, 233–239.
- CHEN, S., FOIAS, C., HOLM, D. D., OLSON, E., TITI, E. S. & WYNNE, S. 1998 Camasa–Holm equations as a closure model for turbulent channel and pipe flow. *Phys. Rev. Lett.* **81** (24), 5338–5341.
- CHEN, S., HOLM, D. D., MARGOLIN, L. G. & ZHANG, R. 1999 Direct numerical simulations of the Navier–Stokes alpha model. *Physica D* **133**, 66–83.
- CONSTANTIN, P. 2001 An Eulerian–Lagrangian approach to the Navier–Stokes equations. *Commun. Math. Phys.* **216**, 663–686.
- CONSTANTIN, P., E, W. & TITI, E. S. 1994 Onsager’s conjecture on the energy conservation for solutions of Euler’s equation. *Commun. Math. Phys.* **165**, 207–209.
- DELROIT, J.-M. 1991 Existence de nappe de tourbillion en dimension deux. *J. Am. Math. Soc.* **4**, 553–586.
- DIPERNA, R. J. & MAJDA, A. J. 1987 Concentrations in regularizations for 2-D incompressible flow. *Commun. Pure Appl. Maths* **40**, 301–345.
- DUCHON, J. & ROBERT, R. 2000 Inertial energy dissipation for weak solutions of incompressible Euler and Navier–Stokes equations. *Nonlinearity* **13**, 249–255.
- EYINK, G. L. 2001 Dissipation in turbulence solutions of 2D Euler equations. *Nonlinearity* **14**, 787–802.
- EYINK, G. L. 2003 Local 4/5-law and energy dissipation anomaly in turbulence. *Nonlinearity* **21**, 1233–1252.
- EYINK, G. L. & SREENIVASAN, K. R. 2006 Onsager and the theory of hydrodynamic turbulence. *Rev. Mod. Phys.* **78**, 87–135.
- FOIAS, C., HOLM, D. D. & TITI, E. S. 2001 The Navier–Stokes-alpha model of fluid turbulence. *Physica D* **152–153**, 505–519.
- FOIAS, C., HOLM, D. D. & TITI, E. S. 2002 The three dimensional viscous Camassa–Holm equations, and their relation to the Navier–Stokes equations and turbulence theory. *J. Dyn. Diff. Equ.* **14**, 1–35.
- HOLM, D. D. 2002 Variational principles for Lagrangian-averaged fluid dynamics. *J. Phys. A* **35**, 679–688.

- HOLM, D. D. & MARSDEN, J. E. 1998 The Euler–Poincaré equations and semidirect products with applications to continuum theories. *Adv. Maths* **137**, 1–81.
- HOLM, D. D., MARSDEN, J. E. & RATIU, T. S. 1998 Euler–Poincaré models of ideal fluids with nonlinear dispersion. *Phys. Rev. Lett.* **80** (19), 4173–4176.
- HOLM, D. D., NITSCHKE, M. & PUTKARADZE, V. 2006 Euler-alpha and vortex blob regularization of vortex filament and vortex sheet motion. *J. Fluid Mech.* **555**, 149–176.
- HOU, T. Y. & LI, C. 2006 On global well-posedness of the Lagrangian averaged Euler equations. *SIAM J. Math. Anal.* **38** (3), 782–794.
- KIMURA, Y. 1987 Similarity solution of two-dimensional point vortices. *J. Phys. Soc. Japan* **56**, 2024–2030.
- KRAICHNAN, R. H. 1967 Inertial ranges in two-dimensional turbulence. *Phys. Fluids* **10**, 1417–1423.
- LEIMKUHLER, B. & REICH, S. 2005 *Simulating Hamiltonian Dynamics*. Cambridge University Press.
- LEITH, C. E. 1968 Diffusion approximation for two-dimensional turbulence. *Phys. Fluids* **11**, 671–672.
- LINSHIZ, J. S. & TITI, E. S. 2010 On the convergence rate of the Euler- α , an inviscid second-grade complex fluid, model to the Euler equations. *J. Stat. Phys.* **138**, 305–332.
- LUNASIN, E., KURIEN, S., TAYLOR, M. A. & TITI, E. S. 2007 A study of the Navier–Stokes- α model for two-dimensional turbulence. *J. Turbul.* **8**, 1–21.
- MARSDEN, J. E. & SHKOLLER, S. 2003 The anisotropic Lagrangian averaged Euler and Navier–Stokes equations. *Arch. Rat. Mech. Anal.* **166**, 27–46.
- MOHSENI, K., KOSOVIĆ, B., SHKOLLER, S. & MARSDEN, J. E. 2003 Numerical simulations of the Lagrangian averaged Navier–Stokes equations for homogeneous isotropic turbulence. *Phys. Fluids* **15** (2), 524–544.
- NEWTON, P. K. 2001 *The N-Vortex Problem, Analytical Techniques*. Springer.
- NOVIKOV, E. A. 1976 Dynamics and statistics of a system of vortices. *Sov. Phys. JETP* **41**, 937–943.
- NOVIKOV, E. A. & SEDOV, Y. B. 1979 Vortex collapse. *Sov. Phys. JETP* **50** (2), 297–301.
- OLIVER, S. & SHKOLLER, S. 2001 The vortex blob method as a second-grade non-Newtonian fluid. *Commun. Part. Diff. Equ.* **26**, 295–314.
- ONSAGER, L. 1949 Statistical hydrodynamics. *Nuovo Cimento Suppl.* **6**, 279–289.
- SHASHIKANTH, B. N. 2010 Dissipative N -point-vortex models in the plane. *J. Nonlinear Sci.* **20**, 81–103.
- SHKOLLER, S. 2001 Smooth global Lagrangian flow for the 2D Euler and second-grade fluid equations. *Appl. Maths Lett.* **14**, 539–543.
- SYNGE, J. L. 1949 On the motion of three vortices. *Can. J. Math.* **1**, 257–270.
- WATSON, G. N. 2008 *A Treatise on the Theory of Bessel Functions*. Merchant Books.